

Just Ramp-up: Unleash the Potential of Regression-based Estimator for A/B Tests under Network Interference

Qianyi Chen¹, Bo Li^{1*}

¹School of Economics and Management, Tsinghua University

cqy22@mails.tsinghua.edu.cn, libo@sem.tsinghua.edu.cn

Abstract

A/B tests on modern platforms, including social networks and two-sided marketplaces, often encounter challenges due to network interference. Recent research in causal inference under network interference has explored various experimental designs and estimation techniques to address this issue. However, existing methods, which typically rely on single experiments, often reach a performance bottleneck and face limitations in handling diverse interference structures. In contrast, we propose leveraging multiple experiments to overcome these limitations. In industry, the use of sequential experiments, often known as the ramp-up process, where traffic to the treatment gradually increases, is common due to operational needs like risk management and cost control. Our approach shifts the focus from operational aspects to the statistical advantages of merging data from multiple experiments. By combining data from sequentially conducted experiments, we aim to estimate the global average treatment effect (GATE) more effectively. In this paper, we begin by analyzing the bias and variance of the linear regression estimator for GATE under general linear network interference. We demonstrate that bias plays a dominant role in the bias-variance tradeoff and highlight the intrinsic bias reduction achieved by merging data from experiments with strictly different treatment proportions. Herein the improvement introduced by merging two steps of experimental data is essential. In addition, we show that merging more steps of experimental data is unnecessary under general linear interference, while it can become beneficial when nonlinear interference occurs. We also provide an intuitive and informative explanation for this significant bias reduction, as well as the synergetic effect between our merging methodology and cluster-level randomization. Furthermore, we look into a more advanced estimator based on graph neural networks (GNN). Through extensive simulation studies¹, including novel and challenging scenarios such as square root interference, multihop interference, and dynamic graph structures, we show that the regression-based estimator benefits remarkably from training on merged experiment data, achieving outstanding statistical performance. Additionally, we also verify that most of our theoretical results and insights derived from linear regression can also be generalized to the GNN-based estimators.

*Corresponding author

¹The code is available at <https://github.com/Cqyiiii/Just-Ramp-up>.

1 Introduction

A/B tests, also known as randomized controlled trials, have been widely adopted by modern online platforms as a paradigm of data-driven decision-making to support rapid product iteration [30, 42]. In most cases, the interested causal estimand is the GATE, since the experimenter is concerned with how much improvement on performance metrics, such as user engagement, would be achieved by introducing a new product feature to all users versus maintaining the status quo. In complex systems like social networks and marketplaces, the classic Stable Unit Treatment Value Assumption (SUTVA) in causal inference is often violated in cases of social interaction and competition, where the outcome of one user is influenced by the treatments of neighboring users. In such scenarios, the challenge of causal inference under interference naturally arises. This interference, mediated through a graph—such as a social network or market bipartite—is called network interference.

Network interference poses a great challenge to the estimation of GATE, since the platform often only allows experiments with a limited proportion of treatment, instead of the targeted global treatment. This practice considers both risk and cost control, especially since new features are proposed constantly and over a thousand new experiments are launched weekly on social platforms like LinkedIn and WeChat, in parallel [70, 39]. Therefore, the treatment proportion is often limited at the initial phase, typically 2% or 5%, and further experiments are implemented only for those promising ones [74, 42, 52, 71], which composes a ramp-up process of treatment proportions. While this ramp-up is primarily for operational reasons, we will discuss the statistical benefits of leveraging earlier, smaller-scale experiments in addition to the experimental data at the current step. Specifically, for GATE estimation, we train a regression model on the merged experimental data to predict the mean outcomes under global treatment/control.

Recently, numerous experimental designs and estimation techniques have been proposed to address network interference, with many restricted to the neighborhood interference assumption. This assumption simplifies the influence of the entire treatment vector on a specific unit to the treatments of its 1-hop neighborhood, providing significant technical convenience and becoming a popular choice for reducing the dimension of the treatment vector. However, spillover beyond the 1-hop neighborhood is both possible and important in practice, necessitating the analysis of more general interference. Nevertheless, the estimation techniques for interference beyond the 1-hop neighborhood remain underexplored. To make the discussion more practical, we first analyze the bias and variance of our regression-based estimator under general linear interference, where the interference is admitted to be pervasive throughout the whole graph.

There has been a series of works studying spatiotemporal interference with panel data [1, 53, 61], which consider estimands different from static setting and usually require stronger assumptions, e.g. factor model. On one hand, there exists a variety of temporal interference in different scenarios [28, 23, 24, 73, 12], while we target developing general methodology. On the other hand, we believe the estimation of static GATE has not yet been solved elegantly, particularly regarding simulation performance. Therefore, we do not consider any temporal interference in the ramp-up process; instead, we focus on network interference and leverage multiple experiments for estimating the static GATE. Nonetheless, our analysis incorporates temporal correlation of treatment assignments, e.g. the staggered rollout

design [41, 3, 73], which ensures temporal monotonicity in the treatment of any specific unit and introduces strong temporal correlation in its treatments over different time points. In addition, we mention that our framework can easily accommodate dynamic graph structure and temporal interference, though the latter is concerned with the change of estimand and out of the scope of this paper.

For estimators, beyond classic Horvitz-Thompson (HT) and difference-in-means estimators, there have been lots of estimators targeting GATE estimation under network interference, such as HT-style estimator based on different exposure mappings [64, 22], Hájek estimator [27, 65], cluster-adaptive estimator [49]. In this paper, we focus on the regression-based estimator for static GATE. Besides, [27] discusses the advantages of regression-based estimators, such as convenience for implementation, and capacity to incorporate covariates. Nonetheless, we emphasize another point: regression on network experiment data actually models the interference effect. Our core methodology, merging experiment data at different steps, can significantly improve the training of such regression models since it augments the training data intrinsically. In contrasts, we will demonstrate that repeating the experiment with the same treatment proportion is much less effective for training regression model.

The key methodology proposed and discussed in this paper is merging data from multiple experiments that are selected from the ramp-up process for training a regression model for predicting unit outcomes. We first develop theoretical results on bias and variance of simple linear regression under general linear interference. We demonstrate that bias dominates when the interference is of regular intensity, and our merging procedure can substantially reduce the bias. However, the bias reduction achieved with the linear regression model remains unsatisfactory due to its simplicity. Considering the predominant role of bias, we then explore an enhanced estimator based on GNN. Through extensive simulation studies, we verify that most of the conclusions derived in the context of linear regression still hold for the GNN-based estimator. Specifically, we verify that the GNN estimator trained on the merged data composed of two steps achieves the state-of-the-art mean squared error (MSE) with balanced bias and standard deviation in linear interference setting, as illustrated in theoretical analysis of linear regression estimator. Moreover, we also validate that merging more than two steps of experimental data can be beneficial under nonlinear interference.

In Figure 1, we illustrate the statistical performance of both the linear regression estimator and the GNN estimator trained on different T -step (merged) datasets. First, we observe a substantial bias reduction when merging data from two or more experiments, compared to the first column, i.e., regression model trained with one-step data with treatment proportion 50%. Second, the standard deviation contributes much less to the MSE than bias, even for a more complex model like the GNN. Finally, despite the GNN’s expressiveness, its performance on a single dataset remains unsatisfactory. However, its potential is unleashed when more experimental data with varying treatment proportions are merged for training. In summary, we attribute this phenomenon to the increased variation in the treatment exposures of units, introduced by merging experiments with different treatment proportions. The augmented treatment exposure variation better fits the two extreme scenarios required in defining GATE, i.e., global treatment/control, and hence leads to enhanced estimation.

We provide a main takeaway: by pooling experimental data with strictly different treatment proportions, we can train a powerful regression model to accurately predict potential outcomes under both global

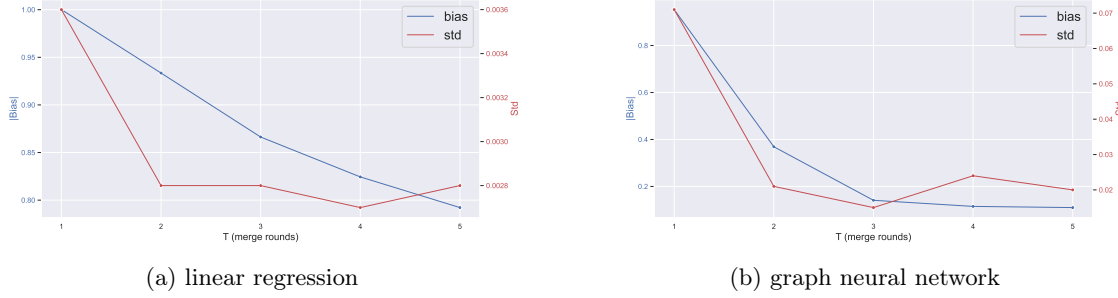


Figure 1: The trajectory of (absolute value of) bias and standard deviation (std) of the regression-based estimators (linear regression and graph neural network) trained on the **merged** T -step experimental data. Here we set the treatment proportions $(c_1, c_2, \dots, c_5) = (2\%, 5\%, 10\%, 25\%, 50\%)$. The t -th column in the figure corresponds to the case that the regression model is trained on merged data with treatment proportions (c_{6-t}, \dots, c_5) . The randomization scheme used here is unit-level complete randomization, and a detailed setting will be introduced in Section 5.

treatment and control. Our proposed methodology is not only effective but also simple. Notably, the ramp-up process is already a standard practice on many platforms, as documented in [74], "every experiment goes through a 'ramp up' process", at LinkedIn. This fact means that our methodology does not require any additional experiment resources, making it a true plug-and-play solution that is easy to implement. We believe our methodology will efficaciously support accurate GATE estimation in the ramp-up process on modern online platforms.

Paper Outline. We begin by introducing the basic setting, as well as the general linear interference model, the default experimental design, and the regression-based estimator. In Section 3, we elaborate on the role of merging for the simple linear regression estimator. Specifically, we demonstrate the dominant place of bias and substantial bias reduction brought by merging. Section 4 provides an intuitive explanation of the effectiveness of our merging methodology, highlighting the increased variation in treatment exposures resulting from merging and offering a novel perspective on cluster-level randomization and its synergistic effect with merging. In Section 5, we conduct an extensive simulation study with the GNN estimator to showcase the remarkable statistical performance achieved by our methodology. Finally, in Section 6, we summarize the paper and discuss related issues.

1.1 Related Works

Causal inference under interference has been studied in early years [62, 57, 36]. Discussion on the most general interference, namely, everyone's outcome can be influenced by the treatment of any other one in an arbitrary way, is nearly meaningless [75]. Thus, we argue that the structure of interference that supports the dimension reduction of the entire treatment vector is necessary for meaningful discussion. As mentioned before, there are two popular structures for static (cross-sectional) data, i.e. social networks and two-sided marketplace. In this paper, we will focus on the interference that is conducted through a concrete and known network structure. There have been many works leveraging bipartite structure in marketplace [55, 77, 14, 6, 33]. The bipartite graphs are typically constructed based on the

demand and supply relation [69, 38, 46, 15, 29]. On one hand, there are situations in which edges are defined as the availability of service, e.g. booking or ridesharing platforms, the graph structure can be highly dynamic as the supply-demand relation changes rapidly. Studying interference in these settings on the basis of a fixed network structure may not be advisable. On the other hand, in situations where edges are defined based a relatively long-term relation, e.g. content subscription, the bipartite structure is deemed to be more stable. Besides, in social network platforms, edges defined as social relations such as friendship can also be viewed as stable at a scale of weeks. The preassumption of fixed network structure is reasonable in a suitable time horizon.

In general, ignoring the interference effect will bias the estimation of GATE severely [54]. Thus, the experimenter should first judge whether there exists considerable interference that necessitates corresponding techniques as countermeasures. Along this direction, a series of tests are proposed to detect the interference effect in various scenarios [4, 56, 31]. After the experimenter confirms the intensity of interference is large enough to be treated carefully, there are mainly two strategies—experimental design and estimation technique, which are before and after the deployment of treatments, respectively. We emphasize that these two strategies are interdependent instead of separate. Before detailed discussion, we first list the common approaches to simplify the interference pattern, which have been adopted in research focusing on either experimental design or estimation.

There has been a stream of research based on the so-called partial interference assumption [62, 36, 10, 25, 17], which posits the network can be partitioned into disjoint groups or clusters and interference only occurs within clusters. This somewhat strong assumption simplifies the interference pattern greatly, wherein cluster-level randomization can easily induce unbiased estimation. A precondition here is that the cluster structure is given in advance, such as geographical zoning. However, such a clean partition of units is almost impossible on the social network. Besides, even the network has a clear cluster structure, between cluster interference may very likely to happen. In classic linear potential outcome models [75, 18] document that the bias is proportional to the number of edges across different clusters.

Without assuming specific network topology such as clustered structure, there are three approaches that aim to restrict the interference to the neighbors of each unit. The first interference pattern, which is more practical and popular in the literature, is neighborhood interference [26, 20, 65, 50]. It assumes the interference is limited to the direct neighbors of each unit. Under this assumption, a unit sharing the same treatment level with all of its neighbors can be considered as being in an environment of global treatment or control, which is ideal for GATE estimation. A classic application of this assumption is the HT estimator with the generalized propensity score. This estimator can achieve unbiasedness without requiring knowledge of the specific form of interference effect, though its variance is likely to be explosive. The second approach is to employ exposure mapping to summarize the impact of the entire treatment vector on a unit through a specific summary function or representation [2, 22, 64, 5, 66], e.g. the proportion of treated neighbors. Besides simple exposure mapping based on domain knowledge, there also exists some recent research targeting learning appropriate exposure mappings from data [76, 63]. Nonetheless, we think the discussion in [60] is valuable, [60] emphasizes separating the two roles of exposure mapping, namely, defining causal estimand of interest and restricting the interference structure, and stress the first one over the second. Thirdly, it is usually non-trivial to analyze bias

and variance of estimator precisely without strong structural assumption, thus another line of work leverages potential outcome model to facilitate such analysis [9, 75, 18]. It is worth noting that these three approaches are not mutually exclusive, and they are somewhat getting stronger progressively. For example, a potential outcome model often implies neighborhood interference or a certain exposure mapping.

Experimental design, also known as randomization scheme, decides the allocation of treatments to units. A classic methodology to tackle network interference is applying cluster-level randomization [36, 64, 65, 34], instead of randomizing at the unit level. Intuitively, cluster-level randomization introduces strong correlations among those units connected densely and creates an environment mimicking global treatment in the interior of the cluster. The clusters are usually formed according to geography characteristics or community detection algorithms on the graph. The first line of work focuses on how to utilize the given cluster structure to construct the optimization problem of experimental design[49, 17, 18], and the other line of work considers how to create better clusters taking into account of the estimation precision metrics such as mean square error (MSE) [44, 68]. As discussed in [18], cluster-level randomization is a good basic scheme that reduces the search space effectively. Nonetheless, unit-level randomization owns its advantage: it is more flexible for implementing certain optimization of experimental design. For instance, min-cut for two-wave experiments [67], max independent set for mimicking global treatment versus global control [16].

There are also abundant estimation techniques developed for causal inference under network interference. The estimation and inference techniques are mainly developed for observational data, where the treatment assignment mechanism is unknown. First, based on partial interference, [48] proposes a generalized inverse probability-weighted estimator and its Hájek-type stabilized weighted estimators, where parametric regression is applied for unknown propensity scores. Second, based on neighborhood interference assumption, [25] consider a joint generalized propensity score (GPS) that incorporates both unit-level treatment and aggregated neighborhood treatments, [26] considers a simplified one removing the exposure part and leverages a Bayesian propensity score adjustment. Such GPS is estimated through logistic regression and penalized spline regression in these two papers, respectively. Finally, GNN has been considered as an more adaptive estimator that goes beyond 1-hop neighborhood and fits the network data naturally. [19] proposes a well-designed architecture for estimating the potential outcomes and propensities in the meanwhile, where GNN is employed to aggregate the covariates as well as the neighborhood interference. [45] considers ANI assumption that further utilizes the ability of GNN to model the general network interference. These papers all focus on observational data, and there are also relatively fewer works considering estimation with experimental data, which is exactly our setting. For example, [32] proposes a regression adjustment method based on sequential feature generation and selection procedures similar to graph convolution. [37] proposes to utilize a mixed experimental design of unit-level and cluster-level randomization to construct a GATE estimator by subtracting two HT estimators calculated on two parts of data admitting different randomization schemes. However, the calculation of such an estimator is concerned with unknown parameters whose number is equal to the number of edges of the graph.

Most of the literature discussed above is based on a single experimental or observational dataset, while

causal inference with multiple datasets is also an interesting topic. We only focus on research leveraging multiple experiments with different treatment proportions. In the following, we compare two related works in similar settings, in detail, which further clarifies the position of our paper.

[20] considers the interference effect characterized by polynomials of treatments of one's 1-hop neighbors and utilizes the multiple experiments with strictly increasing treatment proportion to do Lagrangian interpolation, where treatment proportion acts as the variable. There are two major limitations in this proposal. First, the good performance of Lagrangian interpolation heavily relies on exact knowledge on the order of interaction terms, which is hard to acquire in practice. Second, high-order interaction terms naturally arise for high-degree nodes, requiring larger number of rollout steps to render the interpolation possible. However, in practice, the experiments are typically rolled out in a very few stages due to operational reasons [74]. In contrast, our methodology leverages the known graph structure and does not require any specific domain knowledge; besides, our methodology can provide accurate GATE estimation even with only two rollout stages.

Based on staggered rollout design, [13] proposes a model-selection procedure that implements cross-validation on multiple experimental data to select the best one among potential outcome models that, for instance, define the neighboring units differently. The paper leverages the rollout design to achieve model-based identification of the interference effect and hence can difference out the interference effect based on the model and the resultant identification. The methodology in [13] is developed on the basis of the realizability assumption. That is, they presume the true potential model lies in the considered linear model class. We tend to stick with the "all models are wrong" motto and do not try to tease out the interference effect completely in such a complex setting. Instead, we take a different route and try to showcase the great benefit of bias reduction of training a regression model on the merged experimental data. It is also worthwhile to mention that repeated experiments with the same treatment proportion also suffice for implementing cross-validation in [13], thus rollout design, which concerns strict increasing treatment proportions, is not necessary there. In contrast, our analysis manifests the statistical benefit of merging experimental data with strictly different treatment proportions.

2 Basic Setting

2.1 Preliminary

We adopt the Neyman-Rubin's potential outcome framework [59] and consider a finite population of n units. The treatment vector is represented as $\mathbf{z} = (z_1, z_2, \dots, z_n) \in \{0, 1\}^n$. Without assuming the Stable Unit Treatment Value Assumption (SUTVA), we define the potential outcome of unit i as $Y_i = Y_i(\mathbf{z})$ to account for its possible dependency on the treatments of other units.

The parameter of interest is the global average treatment effect (GATE), which is defined as:

$$\tau := \frac{1}{n} \sum_{i \in [n]} (Y_i(\mathbf{1}) - Y_i(\mathbf{0})) \quad (1)$$

Here, $[n]$ denotes the unit set $\{1, 2, \dots, n\}$, and $\mathbf{1}(\mathbf{0})$ represents the n -dimensional vector of 1(0), corresponding to global treatment and global control, respectively.

We take the network structure as given, defined by an undirected graph $\mathcal{G} = (\mathcal{V}, \mathcal{E})$. For simplicity, we assume this graph \mathcal{G} contains neither loop nor duplicate edges. Here the node set \mathcal{V} is the unit set $[n]$, and edges are characterized by the adjacency matrix A . In addition, we use \deg_i to denote the degree of node i on the graph, and matrix $D = \text{diag}(\deg_1, \deg_2, \dots, \deg_n)$. For convenience, we assume $\deg_i > 0$ holds for all unit $i \in [n]$.

2.2 General Linear Interference Model

We consider the following potential outcome model, which we refer to as the general linear interference model:

$$Y(\mathbf{z}) = \beta_0 + \beta_1 \mathbf{z} + \beta_2 B\mathbf{z} + \epsilon \quad (2)$$

Where β_0 , β_1 , and β_2 are unknown parameters, and we assume $\beta_2 \neq 0$, indicating that there is indeed an interference effect. This model can be written more compactly as:

$$Y(\mathbf{z}) = \begin{pmatrix} \mathbf{1} & \mathbf{z} & B\mathbf{z} \end{pmatrix} \beta + \epsilon \quad (3)$$

We further assume simple Gaussian noise structure to facilitate theoretical analysis.

$$\epsilon \sim N(\mathbf{0}, \sigma_e^2 I_n) \quad \mathbf{z} \perp \epsilon \quad (4)$$

The matrix B in (2) characterizes the interference effects. In this paper, we restrict $B_{ii} = 0$ for all $i \in [n]$ to ensure that β_1 and β_2 accurately represent the direct treatment effect and the interference effect, respectively. For simplicity, we do not assume any heterogeneity in the base effect β_0 and the direct effect β_1 among units. Instead, we put our attention to a general interference matrix B , which is capable of modeling complex long-distance dependencies in the graph. We provide several specific matrices B in the following, which will serve as running examples throughout this paper.

Example 1 (1-hop linear potential outcome model) *If we take $B = D^{-1}A$, then our potential outcome model is reduced to the classic linear model, formatted as follows:*

$$Y_i(\mathbf{z}) = \beta_0 + \beta_1 z_i + \beta_2 \frac{\sum_{j \in \mathcal{N}(i)} z_j}{\deg_i} + \epsilon \quad (5)$$

Here, $\mathcal{N}(i)$ denotes the 1-hop neighborhood of unit i in the graph.

This model is also called as linear-in-means model [2], which is widely analyzed and used for generating potential outcomes in simulation studies. We mention that removing the degree normalization, i.e. setting $B = A$ results in another common case where the exposure condition shifts from the proportion to the number of treated neighbors, thereby characterizing a different class of social interaction.

Example 2 (Multihop linear potential outcome model) We take

$$B = (\mathbf{1}\mathbf{1}^T - I_n) \odot \left(\sum_{m=1}^M r_m (D^{-1}A)^m \right) \quad (6)$$

here \odot is Hadamard product, and $r_1 \geq r_2 \geq \dots \geq r_m > 0$.

Notice that A^m characterizes the m -hop connections on the graph, where A_{ij}^m represents the number of paths of length m connecting units i and j . The term D^{-1} is included here as a normalization factor. The sequence $\{r_i\}_{i=1}^m$ describes how interference decreases with increasing distance on the graph. Additionally, this matrix B also excludes its diagonal elements, which can be viewed as removing the circular effect corresponding to paths that start and end at the same unit i .

Since $D = \text{diag}(A\mathbf{1})$, we can summarize the examples above as $B = g(A)$ for certain function g , namely, B models certain interference that is conducted through the network. We remark that, though our interference model is general enough, it is still linear in treatment vector \mathbf{z} and rules out non-linear components such as interaction terms e.g. $z_i z_j$. We consider the proposed general linear model for carrying out precise bias and variance analysis while maintaining sufficient generality.

2.3 Experimental Design

In this section, we discuss our default experimental design. Specifically, we adopt unit-level *complete randomization* as the basic randomization scheme, which randomly chooses d units from the n units population to receive treatment. To formalize it, we restrict binary treatments $\{z_i\}_{i=1}^n$ to satisfy $\sum_{i=1}^n z_i = d$ besides $\mathbb{E}[z_i] = d/n$ in a single experiment.

We comment that the performance of unit-level complete randomization is often similar to the independent Bernoulli randomization, which assigns treatment to each unit with probability $p = d/n$ independently. However, unit-level complete randomization ensures exactly d treated units, which brings considerable convenience in mathematical derivation, as demonstrated in the Section 3.

We next discuss the setting of multiple experiments. We consider a ramp-up process that includes T experiments that are subject to complete randomization with treated units $d_1 < d_2 < \dots < d_T$. For convenience, we introduce another notation $c_t = d_t/n$. For instance, $T = 5$ and $(c_t)_{t=1}^T = (2\%, 5\%, 10\%, 25\%, 50\%)$, as also illustrated in [74].

Though we separate the n out of d_t here, we remark that all of the derivations in this paper are exact and do not concern the asymptotic issue in high-dimensional statistics. We will employ the asymptotic language solely to highlight the leading terms in complex expressions, and the interested asymptotic regime will be discussed in the Section 3. On one hand, rigorous asymptotic analysis for social networks is more complex than for random graphs, such as the Erdős-Rényi model [47], due to the greater difficulty in characterizing the evolution of a social network as the number of nodes increases. On the other hand, n is usually more than 1 million for modern networks such as that in WeChat and LinkedIn, and even in smaller networks used for simulation studies [58], n is often more than 10,000. Thus, $1/n$ is indeed an ignorable term in contrast to 1.

Since our core methodology is merging multiple experimental data, we will also discuss the selection of T and $(c_t)_{t=1}^T$ in the light of analysis later.

2.4 Regression-based Estimator

We consider the regression-based estimator, which is concerned with a function $f \in \mathcal{F}$ that predicts the potential outcome $Y(\mathbf{z})$. We formulate it as

$$f : \{0, 1\}^n \times \mathcal{A} \rightarrow \mathbb{R}^n \quad (7)$$

where \mathcal{A} is the space of all possible adjacency matrices for an undirected graph with n nodes, no loops, and no duplicate edges.

Given such prediction function f , we have the following GATE estimator

$$\hat{\tau}(f) = \frac{1}{n} \mathbf{1}^T (f(\mathbf{1}, A) - f(\mathbf{0}, A)) \quad (8)$$

In this paper, we will focus on two classes of regression models: linear regression \mathcal{F}_{lr} and graph neural networks \mathcal{F}_{gnn} . Generally, to obtain such functions f , we require a dataset \mathcal{D} for model training, which is formed by selecting from the experimental data collected so far. In the next section, we will also discuss how to construct better training data to unleash the potential of regression-based estimators from a statistical perspective, rather than an operational one. Additionally, $f \in \mathcal{F}_{gnn}$ is well-suited to scenarios where the graph structure is dynamic—such as when the social network topology is updated weekly on online platforms. It is entirely feasible to train a regression model on merged data with varying network topologies, e.g., $(\mathbf{z}_1, A_1), (\mathbf{z}_2, A_2)$.

3 Analysis on Linear Regression Estimator

In this section, we perform a detailed analysis of the simple linear regression model². As will be demonstrated in the subsequent subsections, this regression model provides a clear illustration of the role of merging experimental data for training. Many of the phenomena observed with this simple regression model can also be generalized to other regression models, such as those in \mathcal{F}_{gnn} , which will be discussed in the simulation study. In summary, the linear regression model examined here is both straightforward and sufficiently powerful for illustration, allowing for the development of insightful conclusions. To be specific, the considered linear regression model is given by:

$$Y = X(\mathbf{z})\theta \quad (9)$$

here $X(\mathbf{z}) = (\mathbf{1}, \mathbf{z})$, $\theta = (\theta_0, \theta_1)^T$.

²We refer to it as "simple" because it does not incorporate knowledge of graph topology; that is, $f(\mathbf{z}, A) = f(\mathbf{z})$ for $f \in \mathcal{F}_{lr}$

After estimating $\hat{\theta}$ from the data, our GATE estimator is given by:

$$\hat{\tau} = (\hat{\theta}_1 + \hat{\theta}_0) - \hat{\theta}_0 = \hat{\theta}_1 \quad (10)$$

Linear regression admits a closed-form optimal solution that brings huge technical convenience. Nonetheless, there exists additional complexity lying in the randomness of the design matrix $X(\mathbf{z})$, since it incorporates the randomness of treatment assignment. As is well known, the closed-form solution of ordinary least squares (OLS) is

$$\hat{\theta} = (X(\mathbf{z})^T X(\mathbf{z}))^{-1} X(\mathbf{z})^T Y \quad (11)$$

here we keep the notation $X(\mathbf{z})$ to stress its dependency on experimental design.

The inverse of such a matrix involves a determinant in the denominator, making the analysis intractable if this determinant also incorporates randomness. Therefore, we consider $\dim(\theta) = 2$ and complete randomization scheme in the following analysis.

3.1 One-step Experiment

In this part, we first examine the simplest case in that only one experiment is conducted, i.e. $T = 1$. We specify the number of treated units in the experimental data as $d = cn$ and construct the following conclusion:

Theorem 1 *The bias and variance of the linear regression estimator under general linear interference are given by:*

$$\begin{aligned} \text{Bias}(\hat{\tau}) &= \mathbb{E}[\hat{\theta}_1] - (\beta_1 + \frac{\beta_2}{n} \text{trace}(\mathbf{1}\mathbf{1}^T B)) \\ &= \frac{\beta_2}{nc(1-c)} \text{trace}(\mathbb{E}[\mathbf{z}(\mathbf{z} - c\mathbf{1})^T] B) - \frac{\beta_2}{n} \text{trace}(\mathbf{1}\mathbf{1}^T B) \\ &= -\frac{\beta_2}{n} \left(\sum_{i,j} B_{ij} \right) \left(\frac{1}{n(n-1)} + 1 \right) \end{aligned} \quad (12)$$

and

$$\begin{aligned}
\text{Var}(\hat{\tau})/\beta_2^2 &= \left(\frac{1}{nc(1-c)}\right)^2 \text{Var}((\mathbf{z} - c\mathbf{1})^T B \mathbf{z}) + \frac{1}{(\beta_2 nc(1-c))^2} \mathbb{E}[(\mathbf{z} - c\mathbf{1})^T (\mathbf{z} - c\mathbf{1})] \sigma_e^2 \\
&= \left(\frac{1}{nc(1-c)}\right)^2 \left(\left(\sum_{i,j} B_{ij}\right)^2 \frac{c(d-1)}{(n-1)} \left(\frac{c(d-n) + 6 + 6c^2 - 12c}{(n-2)(n-3)} \right) \right. \\
&\quad + \left(\sum_{i,j,k} B_{ij} B_{kj} \right) \frac{c(d-n) + 2c^2 + 2 - 4c}{(n-1)(n-2)} \\
&\quad + \left(\sum_{i,j,l} B_{ij} B_{il} \right) \left((1-2c)c \frac{(d-1)(d-2)}{(n-1)(n-2)} + c^3 \frac{d-1}{n-1} \right) \\
&\quad + \left(\sum_{i,j} B_{ij}^2 \right) \left((1-2c)c \frac{d-1}{n-1} + c^3 \right) \\
&\quad + \left(\sum_{i,j} B_{ij} B_{ji} \right) (1-c)^2 c \frac{d-1}{n-1} \\
&\quad - \left(\sum_{i,j} B_{ij} \right)^2 \frac{1}{(n(n-1))^2} \\
&\quad \left. + \frac{\sigma_e^2}{\beta_2^2 nc(1-c)} \right)
\end{aligned} \tag{13}$$

The notation such as $\sum_{i,j}$ denotes summation over $i \in [n], j \in [n]$ without additional constraints. The details of the proof are provided in Appendix A.1. We now proceed to elaborate on the results presented above.

First, we notice that the intensity of direct effect, β_1 , does not influence either bias or variance. In fact, only the intensity of interference, β_2 , appears in the expressions above. Then we check the expression of bias, where the part from estimator $\mathbb{E}[\hat{\theta}_1]$ contributes to the increase of bias, even though its order of quantity is much lower than that of relative bias³ induced by interference effect. This implies that the primary source of bias is the interference, while interference term is absent in this linear regression.

The variance seems more complex than the bias. The most intricate part involves the expectation of a squared term, which we expand by categorizing the quadruple (i, j, k, l) scenarios. Specifically, we evaluate the value of the following terms:

$$\mathbb{E}[B_{ij} B_{kl} z_i(z_j - c) z_k(z_l - c)] \tag{14}$$

This naturally raises a discussion on the matrix B . We need to consider the following summation

$$\sum_{(i,j,k,l) \in \mathcal{I}} B_{ij} B_{kl} \tag{15}$$

for certain index set $\mathcal{I} \subseteq [n]^4$. For example,

$$\mathcal{I} = \{(i, j, k, l) \mid i = k, j = l, i \in [n], j \in [n], k \in [n], l \in [n]\} \tag{16}$$

³Hereafter, we use the term relative bias to denote Bias/β_2 .

Notice that we have restricted $B_{ii} = 0$, thus whether $i \neq j$ holds does not matter, and the the summation $\sum_{i,j} B_{ij}^2$ in Theorem 1 corresponds to this index set.

To obtain more insightful results, we choose to control the order of such a complex expression of variance. The key message from the variance analysis is that in the regular case—where interference is neither too weak nor too strong—the variance is negligible compared to the bias in magnitude. To formalize the scenario of interest, we introduce Assumption 1 that limits our analysis to cases of regular interference. Rather than constraining the order of five summations in Theorem 1 separately, we find that it can boil down to three succinct and reasonable conditions.

Assumption 1 (Intensity of regular interference) *Based on the proposed general linear interference model, we further assume that for all $i \in [n]$*

$$\sum_{j=1}^n |B_{ij}| = O(1) \quad (17)$$

Moreover,

$$\sum_{i,j} B_{ij} = \Theta(n) \quad (18)$$

and

$$\sum_j (\sum_i B_{ij})^2 = O(n) \quad (19)$$

Overall, the essence of this regime is to ensure that the interference effect does not overshadow the main treatment effect. Scenarios where interference is excessively strong are relatively rare. Moreover, to assess the relative order of variance compared to bias in such cases, we will inevitably encounter the order of $\sum_{(i,j,k,l) \in \mathcal{I}} B_{ij} B_{kl} / \sum_{i,j} B_{ij}$ for various index sets \mathcal{I} as outlined in Theorem 1. This complexity makes it challenging to derive succinct conclusions without specifying the interference matrix B .

Given the studied regime in Assumption 1, we derive the following corollary:

Corollary 1 *Based on Assumption 1 and Theorem 1, we further conclude that*

$$\begin{aligned} \text{Bias}(\hat{\tau})/\beta_2 &= \Theta(1) \\ \text{Var}(\hat{\tau})/\beta_2^2 &= \Theta(1/n) \end{aligned} \quad (20)$$

The proof of Corollary 1 can be found in Appendix A.2. This corollary asserts that, within the regime of interest, the primary challenge introduced by interference lies in the bias rather than the variance, especially considering that social networks on online platforms are typically large-scale. Therefore, to reduce the MSE effectively, our focus should first be on addressing the bias term.

We then further clarify the implications of Assumption 1. For a specific unit i , the interference on its outcome is represented by $\beta_2 \sum_j B_{ij} z_j$, and the treatment effect is β_1 . The first part of Assumption 1 restricts the interference effect received by unit i to be of constant order, ensuring that interference does not dominate the outcome for unit i . Additionally, this assumption allows for some units to be

minimally affected by interference. At last, through basic algebra, one can verify that $\sum_j |B_{ij}|$ is equal to 1 in Example 1 and less than⁴ $\sum_{m=1}^M r_m$ in Example 2.

The second part of Assumption 1 restricts the order of total interference effect to be regular. While we assume that $\sum_{i,j} B_{ij} = \Theta(n)$, the bias reduction results discussed in the subsequent subsections also apply when $\sum_{i,j} B_{ij} = o(n)$, which indicates very weak interference. We do not incorporate this case here because the bias introduced by interference diminishes as n increases, given that $\sum_{i,j} B_{ij}/n = o(1)$. As illustrated in the expression of bias, it is unnecessary to use specific techniques designed to address interference, in this case. Therefore, we focus on the meaningful and challenging scenario, where $\sum_i B_{ij} = \Theta(n)$. For instance, in the Examples 1 and 2, the order of $\sum_i B_{ij}$ are both $\Theta(n)$.

The final part of Assumption 1 restricts the order of the sum of the total impact that unit i imposes on other units. Intuitively, it restricts the number and influence of highly influential opinion leaders within the network. In Example 1, this assumption does not always hold and thus imposes substantial constraints on the adjacency matrix A , specifically,

$$\mathbf{1}^T D^{-1} A^2 D^{-1} \mathbf{1} = O(n) \quad (21)$$

For instance, in a ring graph, we have $\sum_j (\sum_i B_{ij}) = \Theta(n)$, while in a star graph—where one opinion leader connects to all other units—we have $\sum_j (\sum_i B_{ij}) = \Theta(n^2)$. In the context of Example 1, a sufficient condition for satisfying this assumption is restricting the growth rate to a constant κ , a condition commonly employed in related works [64]. However, a restricted growth rate is not a necessary condition. As a counterexample, consider the complete graph, where $\mathbf{1}^T D^{-1} A^2 D^{-1} \mathbf{1} = n$; despite being the densest graph, it lacks any prominent opinion leaders. We further assert that this assumption is reasonable for typical social networks like WeChat, where, even with over a billion nodes, it is unlikely for any single unit to have more than 100,000 friends while maintaining significant influence over each one of them.

Lastly, the final part of Assumption 1 is not required for deriving the Corollary 1 but is instead intended to support the conclusion in the case of merging data, specifically that the variance of the linear regression estimator remains at the order of $\Theta(1/n)$ and is therefore still negligible.

3.2 Two-step Experiment

Although the derivation with $T > 2$ steps experiment does not introduce special complexity compared to the case of $T = 2$, we discuss the case of $T = 2$ separately because the benefit brought by merging two steps experimental data with strictly different treatment proportion is intrinsic, contrasting the case of single experiment or repeated experiments with the same treatment proportion.

First, we outline the changes induced by merging two experimental datasets. The sample size increases from n to $2n$, and the number of treated units changes from d to $d_1 + d_2$. Correspondingly, the treatment proportions in two experiments are c_1 and c_2 . In linear regression, this additionally leads to

⁴If we do not remove the diagonal elements of $(D^{-1} A)^m$, then we would exactly have $\sum_j |B_{ij}| = \sum_{m=1}^M r_m$.

the following two changes:

$$B \xrightarrow{\text{expand}} \begin{pmatrix} B & 0 \\ 0 & B \end{pmatrix} \quad \mathbf{z} \xrightarrow{\text{expand}} \begin{pmatrix} \mathbf{z}_1 \\ \mathbf{z}_2 \end{pmatrix} \quad (22)$$

Remark. In the change from $T = 1$ to $T = 2$, it can be demonstrated that our analytical framework is flexible enough to incorporate temporal interference and dynamic graph structure. For example, the upper triangular part of the block diagonal matrix $\text{diag}(B, B)$ can characterize very general temporal interference, i.e. the treatment assignment of unit i at first round can linearly affect the outcome of unit j at second round. Nevertheless, temporal interference complicates the definition of GATE and is out of the scope of this paper. For the dynamic graph structure, the case just becomes $\text{diag}(B_1, B_2)$, as we assume the interference matrix B is transformed from the adjacency matrix. We examine the case of dynamic graph structure in the last part of our simulation study.

Then we derive following theorem on the bias term.

Theorem 2 *The bias of linear regression estimator trained on merged data ($T = 2$) under general linear interference is given by*

$$\text{Bias}(\hat{\tau})/\beta_2 = -\frac{\sum_{ij} B_{ij}}{n} \left(1 - \frac{(n-1)(c_1 - c_2)^2 + 2(c_1^2 + c_2^2) - 2(c_1 + c_2)}{(n-1)(c_1 + c_2)(2 - (c_1 + c_2))} \right) \quad (23)$$

We maintain the assumption $c_1, c_2 \in [0, 1]$ and $c_1 < c_2$, as introduced in the Section 2. Through basic algebra, we can verify that

$$1 - \frac{(n-1)(c_1 - c_2)^2 + 2(c_1^2 + c_2^2) - 2(c_1 + c_2)}{(n-1)(c_1 + c_2)(2 - (c_1 + c_2))} > 0 \quad (24)$$

which means training on merged experimental data with treatment proportion c_1 and c_2 can **substantially** reduce the bias, and the reduction on relative bias compared to training on single experimental dataset (with treatment proportion c) is

$$\frac{\sum_{ij} B_{ij}}{n} \left(\frac{(n-1)(c_1 - c_2)^2 + 2(c_1^2 + c_2^2) - 2(c_1 + c_2)}{(n-1)(c_1 + c_2)(2 - (c_1 + c_2))} + \frac{c}{n(n-1)} \right) \quad (25)$$

If we ignore the $O(1/n)$ terms in the expression above, the substantial bias reduction is

$$\frac{\sum_{ij} B_{ij}}{n} \left(\frac{(c_1 - c_2)^2}{(c_1 + c_2)(2 - (c_1 + c_2))} \right) \quad (26)$$

From the perspective of the online platform, $c_1 + c_2$ can be viewed as the total budget to be allocated in the experiment. If we fix $c_1 + c_2$, increasing $|c_1 - c_2|$ corresponds to a decrease in bias. This bias reduction is intuitive, as the estimation of the GATE inherently involves estimating the two mean outcomes with treatment proportions of 0 and 1. Lowering c_1 and increasing c_2 brings us closer to these target mean outcomes. Another way to roughly characterize the budget is to ensure $\max\{c_1, c_2\} \leq c$

since a higher treatment proportion introduces significantly more risk to revenue and/or user experience. In broad terms⁵, the most effective way to reduce bias is setting $c_1 = 0, c_2 = c$. However, even if we set $c_1 = 0, c_2 = c$, the bias becomes:

$$-\frac{\sum_{ij} B_{ij}}{n} \left(1 - \frac{c}{2-c}\right) + O\left(\frac{1}{n}\right) \quad (27)$$

which is still numerically unsatisfactory particularly since $c \leq 0.5$ is common in practice. Moreover, as demonstrated in the next subsection, merging multistep experimental data does not lead to further bias reduction compared to the two-step case. Therefore, we choose to explore more powerful regression models, specifically GNNs, in the later sections.

Moreover, a slightly counterintuitive phenomenon is that repeated experiments with the same treatment proportion c do not lead to bias reduction. Even though the experimental data is generated by sampling a treatment vector \mathbf{z} , and repeated experiments introduce more variation in the treatment exposure of each unit—an aspect that typically enhances regression performance—this does not translate into bias reduction.

Finally, since the derivation and conclusions regarding variance for the case of $T > 2$ are not substantially different from those for $T = 2$, we will defer the detailed results and discussion on variance to the next section. It will be shown that the order of variance remains $\Theta(1/n)$ and thus is still negligible when merging T temporally independent experiments or T rollout experiments.

3.3 T -step Experiment

In this subsection, we present the results for the linear regression estimator based on merged T -step experimental data. As a preview, we first demonstrate that merging multistep experimental data can also bring substantial bias reduction, while it can becomes unnecessary under linear interference, compared to the two-step case. We also establish the theoretical result to show that the variance keeps negligible.

First, we present the bias of the linear regression estimator trained on T -step experimental data.

Theorem 3 *For linear regression estimator trained on merged T -step data, the bias is given by*

$$\text{Bias}(\hat{\tau})/\beta_2 = -\frac{\sum_{ij} B_{ij}}{n} \left(1 - \frac{T \sum_{t=1}^T c_t^2 - (\sum_{t=1}^T c_t)^2}{(\sum_{t=1}^T c_t)(T - \sum_{t=1}^T c_t)}\right) + O\left(\frac{1}{n}\right) \quad (28)$$

Through Cauchy-Schwarz inequality and basic algebra, we can verify that

$$\frac{T \sum_{t=1}^T c_t^2 - (\sum_{t=1}^T c_t)^2}{(\sum_{t=1}^T c_t)(T - \sum_{t=1}^T c_t)} \in (0, 1) \quad (29)$$

⁵In the context of an A/B test, the outcomes under global control (i.e., $c_1 = 0$) are typically known to the platform in advance, as the outcomes of the units of interest are recorded daily or weekly. Thus, there is often no need to experiment with $c_1 = 0$.

Merging data from more than two experiments with varying treatment proportions can still lead to substantial bias reduction compared to the single experiment, similar to the case where $T = 2$.

In machine learning practice, it is common to see that merging more related data enhances the performance of the predictive models. However, through basic algebra, one can verify that merging more experimental data does **not** guarantee further bias reduction. This raises a natural question: Given the completed experiments with treatment proportions $c_1 < c_2 < \dots < c_T$, which new experiment with proportion x will further reduce bias? We address this question through the following corollary.

Corollary 2 *To further reduce the bias, the treatment proportion of new experiment, x , should satisfy*

$$(T^2 C_1 - (T+1)C_1^2 + T C_2) x^2 - ((T-1)C_1^2 + 2TC_1 C_2 + T(T+1)C_2) x + C_1^3 - C_1^2 C_2 > 0 \quad (30)$$

here

$$C_1 = \sum_{t=1}^T c_t \quad C_2 = \sum_{t=1}^T c_t^2 \quad (31)$$

For this quadratic function w.r.t. x , we notice the following two facts about the coefficient of quadratic term and the constant term:

$$\begin{aligned} T^2 C_1 - (T+1)C_1^2 + T C_2 &= (T C_1 (T - C_1)) + (T C_2 - C_1^2) > 0 \\ C_1^3 - C_1^2 C_2 &= C_1^2 (C_1 - C_2) > 0 \end{aligned} \quad (32)$$

We then draw several conclusions about the quadratic function in Corollary 2. First, if $c_1 > 0$, merging data with $x = 0$ —representing data under global control—can always reduce bias. As previously mentioned, this type of data is almost always accessible on online platforms. Second, intuitively, a beneficial proportion x should either be lower than c_1 or higher than c_T , rather than lying within the middle section of $[c_1, c_T]$. This intuition is only for illustration and not rigorous, since x around c_1 or c_T may also bring slight bias reduction, which depends on the specific sequence $(c_t)_{t=1}^T$. Considering the first point discussed above, an effective way to further reduce bias is to conduct a larger-scale experiment, i.e., with $x > c_T$, which can be seen as a no-free-lunch phenomenon.

In addition, we can apply the Corollary 2 in the reverse direction: given the proportions, $\{c_1, \dots, c_T\}$, removing the data with treatment proportion c_t from the merged data set could potentially reduce bias further. Repeating this procedure suggests the final solution would involve merging only the experimental datasets with proportions c_1 and c_T . This outcome underscores the particular significance of the $T = 2$ case, and we will further verify it in the simulation study. Nevertheless, merging multistep experimental data can be beneficial under nonlinear interference, as discussed in Section 5. There, we will also outline the recommended practice for applying our methodology, in conjunction with the results of the simulation study.

While it is theoretically possible to solve an optimization problem to select the treatment proportions $(c_t)_{t=1}^T$ for maximizing bias reduction, we do not recommend this approach. Firstly, the optimization problem is contingent upon the outcome model and the specific regression model used. Although we provide a detailed analysis of the simple regression estimator, it is not typically used in practice.

Secondly, when selecting ramp-up steps in real-world experiments, the experimenter must consider factors such as risk and budget in advance, while such a optimization problem does not capture these practical considerations.

Next, we analyze the variance of the regression-based estimator trained on merged data, which considers the design along the temporal dimension and may introduce an ignorable component. Nevertheless, we conclude that the variance remains of order $\Theta(1/n)$. Given the potential complexity of temporal covariances between treatment vectors \mathbf{z}_{t_1} and \mathbf{z}_{t_2} , we focus on two common scenarios: temporally independent experiments and staggered rollout experiments.

The simpler case is the temporally independent experiments, where $\mathbf{z}_{t_1} \perp \mathbf{z}_{t_2}$ for $t_1, t_2 \in [T]$, $t_1 < t_2$. In this scenario, we have⁶

$$\text{Var} \left(\sum_{t=1}^T (\mathbf{z}_t - \frac{\sum_{k=1}^T c_k}{T} \mathbf{1})^T B \mathbf{z}_t \right) = \sum_{t=1}^T \text{Var} \left((\mathbf{z}_t - \frac{\sum_{k=1}^T c_k}{T} \mathbf{1})^T B \mathbf{z}_t \right) \quad (33)$$

We then utilize following lemma,

Lemma 1 *Given Assumption 1, for a treatment vector \mathbf{z} with treatment proportion $c \in [0, 1]$ and any constant $w \in [0, 1]$, we have:*

$$\text{Var}((\mathbf{z} - w\mathbf{1})^T B \mathbf{z}) = O\left(\frac{1}{n}\right) \quad (34)$$

As a natural consequence, the following theorem on the order of variance is obtained:

Theorem 4 *For the linear regression estimator trained on merged T -step **independent** experimental data, the order of variance is given by*

$$\text{Var}(\hat{\tau})/\beta_2^2 = \Theta\left(\frac{1}{n}\right) \quad (35)$$

The proofs of the lemma and theorem above are provided in Appendix A.6 and A.7.

We then discuss the staggered rollout experiments. Specifically, the rollout experiment enforces the condition that $z_{t_1,i} \leq z_{t_2,i}$ when $t_1 < t_2$, for each unit i . Here, $z_{t_1,i}$ denote the treatment assignment received by unit i during the t_1 -th experiment. Consequently, if $z_{t_1,i} = 1$, it follows that $z_{t_2,i} = 1$, thereby constraining the treatment levels for units with a proportion of c_1 , for any $t_2 > t_1$. This demonstrates the strong temporal correlations among the treatment vectors.

In the context of the rollout experiment, it is essential to acknowledge the following expansion and analyze the order of covariances.

$$\begin{aligned} \text{Var} \left(\sum_{t=1}^T (\mathbf{z}_t - \frac{\sum_{k=1}^T c_k}{T} \mathbf{1})^T B \mathbf{z}_t \right) &= \sum_{t=1}^T \text{Var} \left((\mathbf{z}_t - \frac{\sum_{k=1}^T c_k}{T} \mathbf{1})^T B \mathbf{z}_t \right) \\ &+ 2 \sum_{t_1 < t_2} \text{Cov}[(\mathbf{z}_{t_1} - \frac{\sum_{k=1}^T c_k}{T} \mathbf{1})^T B \mathbf{z}_{t_1}, (\mathbf{z}_{t_2} - \frac{\sum_{k=1}^T c_k}{T} \mathbf{1})^T B \mathbf{z}_{t_2}] \end{aligned} \quad (36)$$

⁶We clarify that the T in the upper right corner of the vector and matrix always represents transposition, in this paper.

Fortunately, within the regime under study, we can still control the variance order, as demonstrated in the following theorem:

Theorem 5 *For the linear regression estimator trained on merged T -step **rollout** experimental data, the order of variance is given by*

$$\text{Var}(\hat{\tau})/\beta_2^2 = \Theta\left(\frac{1}{n}\right) \quad (37)$$

The proof of this theorem is provided in Appendix [A.8](#).

4 Further Intuition: Increase the Variation of Treatment Exposures

In the previous section, we characterized the order of bias and variance across various cases, concluding that bias reduction should be our primary focus. We then demonstrated the effectiveness of bias reduction by merging experimental datasets with distinctly different treatment proportions. In this section, we will use the case of $T = 2$ for illustration.

If the reader closely examines the transition from $T = 1$ to $T = 2$, it becomes clear that the substantial reduction in bias arises from the change in the term $(\mathbf{z} - c\mathbf{1})$ within the bias expression to $(\mathbf{z}_1 - \frac{c_1+c_2}{2}\mathbf{1})$ and $(\mathbf{z}_2 - \frac{c_1+c_2}{2}\mathbf{1})$. Mathematically, the former is zero-mean, which introduces a term of lower order compared to a constant term, whereas the latter two do not. This leads to a natural question: what is the underlying intuition behind this apparent magic, beyond the algebraic transformation? In this section, we aim to provide further insight into the role of merging datasets. Specifically, merging inherently increases the variation in treatment exposures.

In line with the principles of statistical learning⁷, successful model training relies on sufficient variation in the feature space. We note that increasing the variation in covariates X helps reduce the variance of the OLS estimator, $\sigma^2(X^T X)^{-1}$, which represents the classical case where unbiasedness is achieved. However, as shown in Section [3](#), under regular interference, the primary challenge lies in the bias term. Generally, greater variation in data can also reduce the bias of the machine learning model. For instance, in the Ridge regression, increasing data variation can not only reduce variance but also decreases bias. Similarly, in kernel regression with a Gaussian kernel, clustered data points result in a less informative kernel matrix, where most entries approach 1. This limits model flexibility and increases bias.

We will further use Example [1](#) for illustration. In this classical model, the treatment exposure of unit i is specified as the proportion of its treated neighbors:

$$e_i = \frac{\sum_{j \in \mathcal{N}(i)} z_j}{\deg_i} \quad (38)$$

In Example [1](#), we claim that the key challenge in modeling the interference effect is ensuring adequate

⁷As will be demonstrated in the simulation study, merging experimental data with different treatment proportions may not only fail to improve traditional estimators, such as the HT estimator and the difference-in-means estimator but can even degrade their performance.

variation in treatment exposures $\{e_i\}_{i=1}^n$. Fortunately, the generation of e_i involves randomization, which naturally introduces variation. We present the histogram of treatment exposures under a complete randomization⁸ with a treatment proportion of $c = 0.5$.

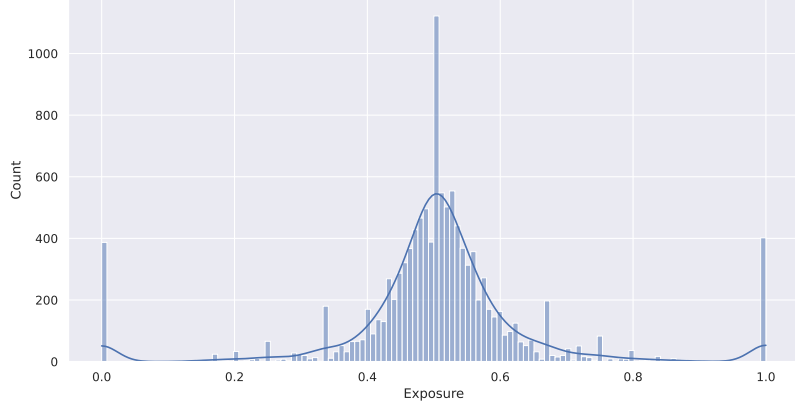


Figure 2: The distribution of treatment exposures under complete randomization with a treatment proportion of $c = 0.5$ is presented. The variance of treatment exposures is 0.0243. The network topology is sourced from the FB-Stanford3 dataset in [58], which represents a Facebook social network comprising $|\mathcal{V}| = 11586$ nodes and $|\mathcal{E}| = 568309$ edges. This network will be used in our simulation study.

Intuitively, the distribution of e_i should be binomial, centered at $c = 0.5$. However, the challenge of the network interference problem lies in the network topology. This distribution can be viewed as the mixture of $\text{Binom}(\deg_i, 1/2)$ of every node i , while $\{\deg_i\}_{i \in \mathcal{V}}$ are interdependent. Additionally, for a node i with $\deg_i = 1$, the treatment exposure e_i is restricted to $\{0, 1\}$, creating two columns at the boundaries of interval $[0, 1]$, as illustrated in Figure 2. In this fully-connected network, there are 494 nodes with $\deg_i = 1$. Moreover, other nodes with low degrees also contribute to these two boundary columns. The cases where $e_i = 1$ and $e_i = 0$ are of particular interest, as they not only directly correspond to the desired global treatment and control conditions but also significantly contribute to the variation in $\{e_i\}_{i=1}^n$.

Next, we present two histograms from the case $c_1 = 0.25, c_2 = 0.5$ in Figure 3. It is evident that the variation in exposures within the merged data increases significantly. Numerically, the variance of treatment exposures with $c = 0.5$ is 0.0243, and such variance with $c = 0.25$ is 0.0188. In the merged data, this variance increases to 0.0377. Beyond the variation introduced by randomization, merging data with different treatment proportions naturally enhances the variation of exposures.

Moreover, we note that the conclusion in Corollary 2 can also be explained by this intuition. For example, the variance of treatment exposures of merged data with treatment proportions (10%, 50%) is 0.0587. However, when we insert another experimental data with $c = 0.25$, the variance of treatment exposures decreases to 0.0459. This corresponds to an increase in bias when experimental data with a treatment proportion x lying in the middle range of $[c_1, c_T]$ is further merged. Similarly, the maximum

⁸All of the histograms presented in this section are based on a single randomization with a fixed random seed.

variance is achieved when exactly 50% treatment exposures are at 0 and 1, respectively. This represents the optimal scenario for GATE estimation, albeit impractical.

To further validate this intuition, we present the distribution of treatment exposure under cluster-level complete randomization in Figure 4. Clearly, the variation of treatment exposure increases significantly compared to that observed in the unit-level randomization. Numerically, the variance of $\{e_i\}_{i=1}^n$ rises to 0.0712.

Cluster-level randomization can be understood in various ways, such as creating an environment that mimics global treatment or control for the units within clusters, or providing strong correlations among treatments according to network topology. Since strong correlations typically lead to increased variance, we note that the latter perspective aligns with the viewpoint of this paper: namely, that increased variation in treatment exposures enhances the performance of regression-based estimators. Although the figures presented are based on a specific form of exposure, we argue that this intuition is applicable to the more general case where $e_i = h_i(\mathbf{z}, A)$ with a non-trivial⁹ function h_i .

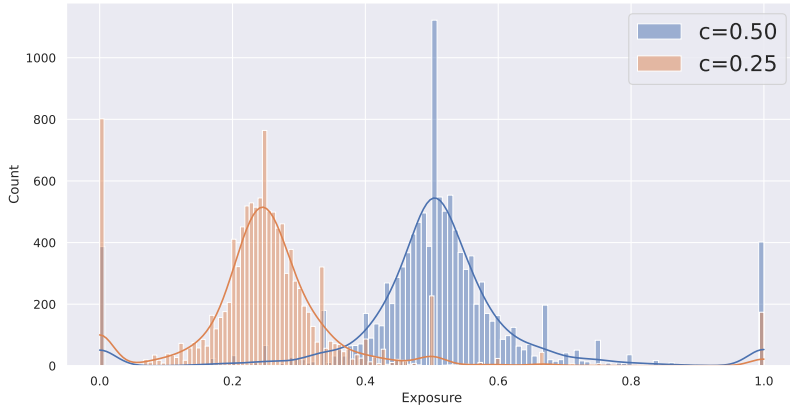


Figure 3: Distributions of treatment exposures under complete randomization with treatment proportion $c = 0.25$ and $c = 0.5$. The variances of treatment exposures are 0.0188 and 0.0243, respectively, with a variance of 0.0377 for the merged data.

Finally, we present the bias and standard deviation of the linear regression estimator and graph neural network estimator under cluster-level randomization in Figure 5, in comparison to Figure 1. We observe a beneficial collaborative effect of the two methodologies that increase the variation of treatment exposures, i.e. merging and cluster-level randomization, which is exactly the recommended practice of our paper. For instance, in one randomization, the variances of treatment exposures in five (merged) data are 0.0709, 0.0784, 0.0810, 0.0781, 0.0728, respectively, corresponding to five columns in Figure 5.

We note that the mechanisms behind both cluster-level randomization and the regression-based estimator are more complex than this intuition suggests¹⁰. Nonetheless, we believe this perspective provides

⁹Here, "non-trivial" refers to the case where the interference effect genuinely depends on the treatment vector and network topology, as opposed to scenarios, for instance, h_i is a constant function.

¹⁰For example, cluster-level randomization benefits not only regression-based estimators but also traditional HT estimators and difference-in-means estimators.

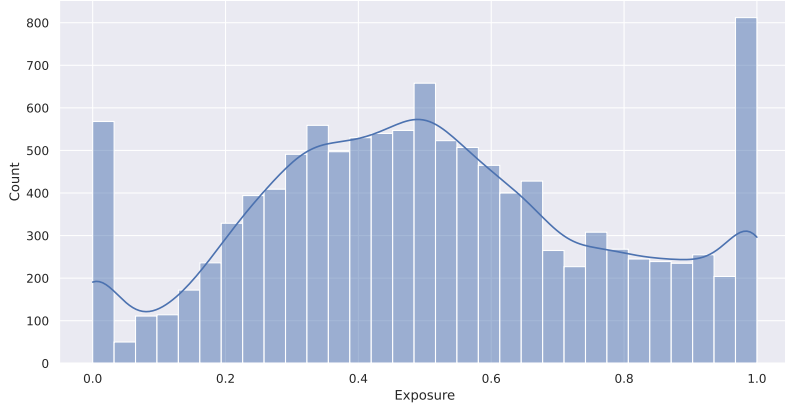


Figure 4: Distribution of treatment exposures under cluster-level complete randomization with treatment proportion $c = 0.5$. The variance of treatment exposures is 0.0712.

valuable insight into the phenomena discussed in this paper, as variation is essential for successful model training.

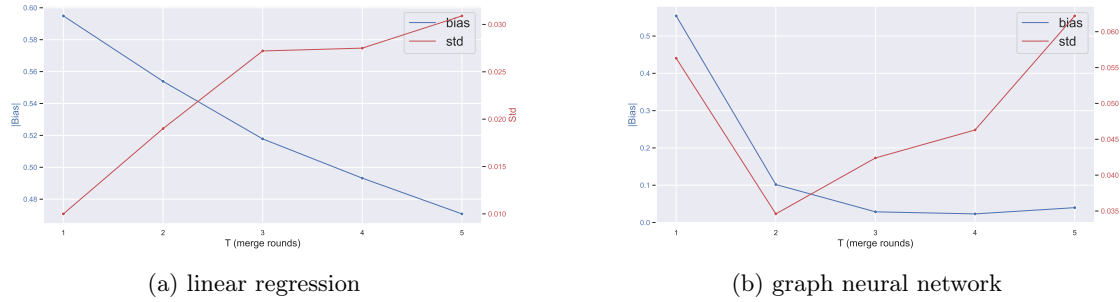


Figure 5: The trajectory of bias and standard deviation (std) of the regression-based estimator (linear regression and graph neural network) trained with **merged** T -step experimental data, which are generated by *cluster-level* complete randomization. The setting is the same as that of Figure 1.

Remark. The mathematical analysis of the variance of $\{e_i\}_{i=1}^n$ in our general linear interference model involves evaluating:

$$\text{trace} (B^T B \text{Cov}[\mathbf{z}]) \quad (39)$$

for a single experiment, and

$$\text{trace} \left(B^T B \left(\sum_{t=1}^T (\mathbf{z}_t - \frac{\sum_{k=1}^T c_k}{T})(\mathbf{z}_t - \frac{\sum_{k=1}^T c_k}{T})^T \right) \right) \quad (40)$$

for T -step experiment. Regretfully, these terms are concerned with the elements of second order term $B^T B$ for specific interference matrix B and the network topology A behind, which complicates deriving useful conclusions, such as the monotonicity with respect to the number of steps merged, T . This

contrasts with the discussion of variance, where we only need to establish conclusions about the order. Therefore, we position this section as providing informative intuition.

5 Simulation Study

5.1 Basic Setting

We begin by outlining the setup of our simulation study. Rather than using a simple random graph, we utilize a Facebook social network FB-Stanford3¹¹ [58], which has also been employed in semi-synthetic experiments in [65, 18]. The network topology \mathcal{G} consists of $|\mathcal{V}| = 11586$ nodes and $|\mathcal{E}| = 568309$ edges, where each node represents a person, and the edges indicate friendships or social relationships. Based on this real network, we generate the potential outcomes with specific models in the subsequent sections to validate the effectiveness of our methodology.

We choose the Chebyshev Spectral Graph Convolution (ChebConv) [21] as our regression model, implemented through the Deep Graph Library [72]. Our GNN model consists of three ChebConv layers, with the detailed parameters of the network architecture provided in Appendix B. We optimize the GNN using the Adam optimizer [40], ensuring that all models are adequately trained to converge, achieving a final training loss below 0.2 across most cases.

The main randomization scheme discussed in this section is complete randomization, which is a basic and widely used one. We will present all of the results with both unit-level and cluster-level randomization. For cluster-level randomization, we apply the Louvain algorithm [11] to generate clusters, with a fixed random seed. This popular community detection algorithm is favored for its low computational complexity and effectiveness. We set the resolution of the clustering algorithm to 10, resulting in 192 clusters. For a discussion on the impact of different clustering resolutions, refer to [18].

Furthermore, the reported bias and standard deviation are calculated through Monte Carlo simulation. We implement the treatment allocations with 1,000 repetitions, corresponding to 1,000 continuous random seeds that control the randomization.

Next, we outline the structure of our simulation study. In the first part, we aim to verify that the conclusions drawn for linear regression also hold for the GNN model, demonstrating the generality of our insights. In the subsequent parts, we extend the study to more complex potential outcome scenarios, including a multiplicative model that falls outside the scope of our general linear interference framework, a quadratic and square root interference term that challenge extrapolation, a multihop interference model that goes beyond classic neighborhood interference assumption, and a dynamic graph structure setting that corresponds to practical, general scenarios. The last three of them are novel in the simulation studies of related works.

¹¹The network topology data can be found in <https://networkrepository.com/socfb-Stanford3.php>

5.2 Basic Simulation under Linear Interference

In this section, we present the bias, standard deviation, and MSE of the GNN model trained on merged experimental data. We adopt the treatment proportions $(c_1, c_2, c_3, c_4, c_5) = (2\%, 5\%, 10\%, 25\%, 50\%)$ in the ramp-up process and consider the training data composed by $t = 1, 2, 3, 4, 5$ steps, corresponding to the treatment proportions (c_{6-t}, \dots, c_5) . Thus, the maximal treatment proportion is fixed at 50%, and we will demonstrate how merging experimental data from earlier ramp-up steps can unleash the potential of GNN model in the task of GATE estimation.

To begin, we design a $2 \times 2 \times 2$ grid of settings. For the randomization level, we consider both unit-level and cluster-level randomization. For the randomization scheme, we explore independent Bernoulli randomization and complete randomization. Lastly, for the temporal dependency of treatment allocations, we consider temporally independent experiments and staggered rollout experiments.

The first generation mechanism of potential outcomes is the classic linear potential outcome model, as described in Example 1.

$$Y_i(\mathbf{z}) = \beta_0 + \beta_1 z_i + \beta_2 \frac{\sum_{j \in \mathcal{N}(i)} z_j}{\deg_i} + \epsilon_i \quad (41)$$

where $\epsilon_i \sim N(0, \sigma_e^2)$ are i.i.d. noises. We set the parameters as $(\beta_0, \beta_1, \beta_2, \sigma_e) = (1, 1, 1, 0.1)$, and the true GATE is $\beta_1 + \beta_2 = 2$.

Table 1: The statistical performance of GNN estimator with **independent Bernoulli randomization** and **temporal independence**

level metric rounds	Unit			Cluster		
	Bias	Std	MSE	Bias	Std	MSE
$t = 1$	-0.945	0.071	0.899	-0.562	0.058	0.320
$t = 2$	-0.365	0.023	0.133	-0.118	0.046	0.016
$t = 3$	-0.142	0.015	0.020	-0.038	0.041	0.003
$t = 4$	-0.115	0.024	0.014	-0.032	0.050	0.004
$t = 5$	-0.110	0.019	0.012	-0.042	0.056	0.005

Table 2: The statistical performance of GNN estimator with **independent Bernoulli randomization** and **staggered rollout**

level metric rounds	Unit			Cluster		
	Bias	Std	MSE	Bias	Std	MSE
$t = 1$	-0.944	0.072	0.896	-0.560	0.058	0.317
$t = 2$	-0.365	0.022	0.134	-0.117	0.047	0.016
$t = 3$	-0.142	0.015	0.020	-0.036	0.044	0.003
$t = 4$	-0.116	0.023	0.014	-0.033	0.051	0.004
$t = 5$	-0.110	0.019	0.012	-0.042	0.056	0.005

We present the results from Table 1 to Table 4. First, we observe that the differences between cluster randomization and independent Bernoulli randomization, as well as between temporally independent

Table 3: The statistical performance of GNN estimator with **complete randomization** and **temporal independence**

level metric rounds	Unit			Cluster		
	Bias	Std	MSE	Bias	Std	MSE
	$t = 1$	-0.953	0.071	0.914	-0.560	0.059
$t = 2$	-0.369	0.021	0.136	-0.114	0.037	0.014
$t = 3$	-0.141	0.015	0.020	-0.033	0.045	0.003
$t = 4$	-0.115	0.024	0.014	-0.031	0.047	0.003
$t = 5$	-0.110	0.020	0.013	-0.042	0.054	0.005

Table 4: The performance of GNN estimator with **complete randomization** and **staggered rollout**

level metric rounds	Unit			Cluster		
	Bias	Std	MSE	Bias	Std	MSE
	$t = 1$	-0.951	0.071	0.909	-0.561	0.059
$t = 2$	-0.369	0.021	0.136	-0.112	0.037	0.014
$t = 3$	-0.142	0.014	0.020	-0.034	0.044	0.003
$t = 4$	-0.116	0.023	0.014	-0.030	0.048	0.003
$t = 5$	-0.110	0.020	0.013	-0.042	0.054	0.005

experiments and staggered rollout experiments, are minimal. The only significant factor in this setting grid is the distinction between unit-level and cluster-level randomization.

Next, similar to the linear regression estimator, the bias remains the dominant factor for the GNN model in most cases. Even for cluster-level randomization and merged rounds where $t \geq 3$, the bias is as significant as the standard deviation. This observation confirms and reinforces the claim regarding the dominance of bias, which was established for the linear regression estimator in the previous sections.

Moreover, we find that although GNN can be viewed as a much more powerful model compared to the simple linear regression, the statistical performance of the estimate given by GNN that is trained on a single experimental data with treatment proportion $c_5 = 50\%$ is not significantly better than linear regression. We first focus on the case of $t = 1$ in the following discussion. For the unit-level randomization, we can compare GNN with linear regression, as previously shown in Figure 1. The bias of the linear regression estimator is exactly -1 because it can not model the interference, in contrast to the bias -0.951 of the GNN estimator, taking Table 4 as example. This result may seem counterintuitive but can be explained by our proposed intuition: the training of model requires sufficient variation in treatment exposure. Furthermore, we observe that the cluster-level randomization can significantly improve the performance of the GNN estimator, as also presented in Figure 5.

However, such a bias of -0.561 remains unsatisfactory. As shown in [18], the basic HT estimator can achieve a bias of -0.588 and standard deviation 0.584, under the same setting and randomization scheme. The intrinsic improvement is brought by merging experimental data in the previous ramp-up steps. Consistent with the discussion for linear regression estimator, the change from $t = 1$ to $t = 2$ introduces

essential bias reduction. When it comes to the case of $t = 3$, the bias of the GNN estimator is further reduced significantly, accompanied by low variance. To summarize, our methodology contributes to an extremely small MSE in this problem setting, especially for cluster-level randomization.

These numerical experiments demonstrate that the GNN, as a powerful function approximator on the graph, has the potential to accurately extrapolate the mean outcome under global treatment. However, effective data-centric engineering—such as merging experimental data with different treatment proportions in our context—is essential to fully leverage the capabilities of this model.

We then consider some basic extensions. We have demonstrated that the difference between cluster randomization and independent Bernoulli randomization, as well as temporally independent experiments and staggered rollout experiments, is very small. Therefore, we will consider a staggered rollout design and complete randomization in all of the simulation studies below.

First, a natural question arises: Is the observed improvement solely due to the increased volume of training data? To address this, we present the result from t repeated experiments, where the treatment proportion of each experiment is set to 50%.

Table 5 shows that the benefits of merging data from repeated experiments are minimal. However, for $t \geq 3$, there is a slight improvement, which can be attributed to the increased natural variation in treatment exposures caused by the randomness of treatment allocation in finite samples¹². Thus, we conclude that substantial bias reduction is achieved by merging experimental data with **different** treatment proportions, which is consistent with the conclusions for linear regression presented in Theorems 2 and 3.

Table 5: The performance of GNN estimator with **repeated experiments**

level metric rounds	Unit			Cluster		
	Bias	Std	MSE	Bias	Std	MSE
	$t = 1$	$t = 2$	$t = 3$	$t = 4$	$t = 5$	
	-0.997	0.013	0.994	-0.600	0.018	0.360
	-0.995	0.012	0.990	-0.599	0.018	0.359
	-0.989	0.015	0.978	-0.595	0.020	0.354
	-0.975	0.025	0.952	-0.583	0.026	0.341
	-0.951	0.071	0.909	-0.561	0.059	0.318

Moreover, as stated in Corollary 2 and discussed therein, we asserted that it is sufficient to merge data with only the lowest and highest treatment proportions, i.e., c_1 and c_T , despite the potential benefits of variance reduction. To examine this claim, we also evaluate the performance of the GNN estimator with $c_1 = 0.02$ and $c_2 = 0.5$, as presented in Table 6.

The results are consistent with the discussion in Corollary 2, indicating that better performance can be achieved by merging data with only the treatment proportions c_1 and c_T . Therefore, we recommend the following best practice for our methodology: train the regression model on merged data with global control and the highest treatment proportion available during the ramp-up phase. In light of this

¹²For instance, if the treatment exposure e_i has a probability of 0.8 of being 0.5 and 0.1 of being 0 or 1, corresponding to the global control/treatment, a larger sample size ensures that the cases where $e_i = 0$ or $e_i = 1$ do occur.

Table 6: The performance of GNN estimator with 2-step experiments and $c_1 = 0.02, c_2 = 0.5$.

level metric rounds	Unit			Cluster		
	Bias	Std	MSE	Bias	Std	MSE
$t = 2$	-0.108	0.015	0.012	-0.022	0.031	0.001

phenomenon, we also evaluated performance with $c_1 = 0$ and varying c_t , as shown in Table 7.

Table 7: The performance of GNN estimator with merged data of $c_1 = 0$ and different c_t .

level metric proportion	Unit			Cluster		
	Bias	Std	MSE	Bias	Std	MSE
$c_t = 0.02$	-0.526	0.034	0.278	-0.216	0.173	0.076
$c_t = 0.05$	-0.369	0.025	0.137	-0.032	0.121	0.016
$c_t = 0.10$	-0.299	0.028	0.090	-0.010	0.130	0.017
$c_t = 0.25$	-0.155	0.020	0.025	-0.037	0.045	0.003
$c_t = 0.50$	-0.092	0.015	0.009	-0.015	0.033	0.001

The most notable observation in this table is that we can achieve a bias of -0.526 for unit-level randomization and -0.216 for cluster-level randomization with $c_t = 0.02$, simply by merging the existing data under global control. Generally, $c_t = 0.02$ represents the earliest stage of the ramp-up process, yet our methodology allows for a significantly accurate estimation of GATE.

Furthermore, if cluster-level randomization is employed and the ramp-up process has reached the stage of $c_t = 0.05$, the bias is only -0.032 , which is two orders of magnitude smaller than the signal scale, i.e., β_1 and β_2 . Although the standard deviation remains 0.121, which is still notable, the GATE estimate at this stage can be considered credible. Finally, for $c_t = 0.5$, the performance reaches a state-of-the-art level compared to settings where only base levels and outcomes under c_T are available, as far as we know.

Remark. Traditional estimators often do not effectively utilize the known base level β_0 , i.e., the potential outcome under global control. For instance, base levels do not impact the difference-in-means estimator, and common adjustments for various HT estimators involve subtracting the base levels when they are known [75, 18].

Finally, we present the performance of the standard HT estimator, which *naively* utilizes the merged data, in Table 8. Specifically, the standard HT estimator provides the following estimates of the treatment effect:

$$\hat{\tau}_{\text{HT}} = \frac{1}{n} \sum_{i \in [n]} \left(\left(\frac{z_i}{\mathbb{E}[z_i]} - \frac{(1 - z_i)}{\mathbb{E}[1 - z_i]} \right) Y_i(\mathbf{z}) \right) \quad (42)$$

Given experimental data with treatment proportions c_1, \dots, c_T , we average T such HT estimators to obtain:

$$\hat{\tau}_{\text{naive-HT}} = \frac{1}{nT} \sum_{t \in [T]} \sum_{i \in [n]} \left(\left(\frac{z_{t,i}}{c_t} - \frac{(1 - z_{t,i})}{1 - c_t} \right) Y_i(\mathbf{z}_t) \right) \quad (43)$$

We observe that averaging over merged data does not affect the estimates when unit-level randomization is used. However, while there is some bias reduction when merging additional data with cluster-level randomization, the increasing standard deviation due to heterogeneity becomes unacceptable. Therefore, we conclude that our methodology is likely to benefit only the regression-based estimator.

Table 8: The performance of HT estimator with merged data with treatment proportions (c_{6-t}, \dots, c_5)

level metric rounds	Unit			Cluster		
	Bias	Std	MSE	Bias	Std	MSE
	$t = 1$	-1.000	0.004	1.001	-0.537	0.503
$t = 2$	-1.000	0.003	1.000	-0.493	0.534	0.528
$t = 3$	-1.000	0.003	1.000	-0.451	0.642	0.615
$t = 4$	-0.999	0.003	0.999	-0.423	0.797	0.814
$t = 5$	-0.999	0.003	0.998	-0.435	0.959	1.108

In summary, we first examine the effectiveness of our methodology in classic linear interference through extensive simulation studies. We then verify the conclusions and insights derived from linear regression estimator before and demonstrate the generality of them. Specifically, our methodology enables the GNN estimator to achieve amazing performance even in experiments with very low treatment proportions, corresponding to the early stages of the ramp-up process.

In the following sections, we will examine the efficacy of our methodology in more challenging settings, and many of which are novel in related works. For comparison, we will keep the default setting that treatment proportions are $(c_1, c_2, \dots, c_5) = (2\%, 5\%, 10\%, 25\%, 50\%)$ in the ramp-up process. For the merging operation, we will consider the two The first case corresponds to the training data composed by $t = 1, 2, 3, 4, 5$ steps, corresponding to the treatment proportions (c_{6-t}, \dots, c_5) . This case is designed to examine the influence of merging more data at previous steps. The second case corresponds to the training data composed of two steps—global control and c_t for increasing t . This case is designed to examine how well we can do in each stage of the ramp-up process. Additionally, we will continue to use complete randomization with staggered rollout.

5.3 Multiplicative Potential Outcome Model

First, we consider the **multiplicative** potential outcome model, which differs from traditional linear interference and is used in [65, 18].

$$Y_i(\mathbf{z}) = (\beta_0 + \epsilon_i) \cdot \frac{\deg_i}{\bar{\deg}} \cdot (1 + \beta_1 z_i + \beta_2 \frac{\sum_{j \in \mathcal{N}_i} z_j}{\deg_i}) \quad (44)$$

Here, $\bar{\deg}$ is the average degree among units, and $\epsilon \sim N(0, \sigma_e^2)$ are i.i.d. noises. Similar to previous section, we set $(\beta_0, \beta_1, \beta_2, \sigma_e) = (1, 1, 1, 0.1)$, and the true GATE is $\beta_0(\beta_1 + \beta_2) = 2$. We first present the result in Table 9.

We observe that the pattern in the multiplicative model is more complex than in the classic linear model.

Table 9: The performance of GNN estimator with **multiplicative** model

level metric rounds	Unit			Cluster		
	Bias	Std	MSE	Bias	Std	MSE
$t = 1$	-1.078	0.039	1.163	-0.811	0.046	0.659
$t = 2$	-0.257	0.037	0.068	-0.122	0.089	0.023
$t = 3$	-0.061	0.077	0.010	-0.058	0.115	0.017
$t = 4$	-0.110	0.106	0.023	-0.003	0.137	0.019
$t = 5$	-0.120	0.104	0.025	-0.118	0.125	0.030

Initially, the performance of the GNN estimator with a single experiment at $c = 0.5$ is unsatisfactory. However, merging experimental data from $t = 2$ or 3 steps can lead to significant improvements. Conversely, as t continues to increase, the MSE rebounds, indicating that merging more data with increased heterogeneity may be counterproductive or even detrimental. Generally, $t = 2$ and $t = 3$ are preferred options. For comparison, the HT estimator with treatment proportion $c = 0.5$ achieves a bias of -0.744 and a standard deviation of 0.274 in the same setting [18].

In light of the discussion above, we further examine the performance when merging only 2-step experiments with $c_1 = 0$ and varying c_2 , as shown in Table 10.

Table 10: The performance of GNN estimator with **multiplicative** model and merged data of $c_1 = 0$ and different c_t .

level metric proportion	Unit			Cluster		
	Bias	Std	MSE	Bias	Std	MSE
$c_t = 0.02$	-1.275	0.055	1.629	-1.103	0.288	1.299
$c_t = 0.05$	-0.959	0.082	0.927	-0.666	0.249	0.505
$c_t = 0.10$	-0.681	0.082	0.471	-0.340	0.205	0.157
$c_t = 0.25$	-0.321	0.098	0.113	-0.193	0.111	0.050
$c_t = 0.50$	-0.164	0.058	0.030	-0.101	0.063	0.014

Similarly, merging two experiments—one with global control and the other with treatment proportion c_T —is sufficient to achieve outstanding performance in this case. Furthermore, the results in Table 11 also validate the synergistic effect of merging data and using cluster-level randomization.

5.4 Quadratic and Square Root Interference Term

Next, we consider the basic linear interference model with two nonlinear cases of interference. Specifically, we first examine the **quadratic** interference term [20], i.e.

$$Y_i(\mathbf{z}) = \beta_0 + \beta_1 z_i + \beta_2 \left(\frac{\sum_{j \in \mathcal{N}(i)} z_j}{\deg_i} \right)^2 + \epsilon_i \quad (45)$$

The quadratic interference term indicates that the marginal benefit of allocating more treatments increases constantly, making extrapolation more challenging. We set $(\beta_0, \beta_1, \beta_2, \sigma_e) = (1, 1, 1, 0.1)$, so the true GATE remains $\beta_1 + \beta_2 = 2$. The results for our default setting are presented in Table 11, and the results with 2-step merged data, where $c_1 = 0$ and c_T is varied, are shown in Table 12.

Table 11: The performance of GNN estimator with **quadratic** interference term

level metric rounds	Unit			Cluster		
	Bias	Std	MSE	Bias	Std	MSE
	$t = 1$	$t = 2$	$t = 3$	$t = 4$	$t = 5$	
	-0.976	0.044	0.955	-0.583	0.063	0.344
	-0.475	0.020	0.226	-0.240	0.040	0.059
	-0.443	0.010	0.196	-0.284	0.038	0.082
	-0.460	0.015	0.211	-0.301	0.044	0.093
	-0.442	0.032	0.196	-0.241	0.064	0.062

Table 12: The performance of GNN estimator with **quadratic** interference term and merged data of $c_1 = 0$ and different c_t .

level metric proportion	Unit			Cluster		
	Bias	Std	MSE	Bias	Std	MSE
	$c_t = 0.02$	$c_t = 0.05$	$c_t = 0.10$	$c_t = 0.25$	$c_t = 0.50$	
	-0.932	0.067	0.874	-0.776	0.120	0.617
	-0.924	0.032	0.855	-0.739	0.084	0.554
	-0.868	0.021	0.754	-0.692	0.074	0.484
	-0.721	0.023	0.520	-0.569	0.058	0.327
	-0.512	0.010	0.262	-0.373	0.035	0.140

We first observe that the quadratic interference term indeed introduces a challenge to the GATE estimation. In this context, the MSE achieved with cluster-level randomization remains numerically acceptable, whereas the MSE with unit-level randomization is unsatisfactory. Furthermore, merging data with $t > 2$ steps is beneficial in this setting. Lastly, we supplement that the standard HT estimator achieves a bias of -0.537 and a standard deviation of 0.485 under cluster-level complete randomization with treatment proportion $c = 0.5$.

Remark. The quadratic interference scenario is the only case in which the best performance of the GNN estimator still results in a bias larger than 0.2. However, this bias, observed in cluster-level randomization and multi-step experimental data, can be easily reduced by increasing the number of parameters, albeit at the cost of slightly higher variance. For instance, if we increase the number of filters in the GNN architecture from $(2, 1, 1)$ to $(2, 4, 2)$, the performance triplet (Bias, Std, MSE) improves to $(-0.166, 0.091, 0.036)$. In fact, the approximation error can be effectively reduced by enlarging the volume of parameter of the GNN model, despite issues related to the expressiveness of the GNN model. However, the performance of GNN estimator with $t = 1$ would become much worse due to limited amount of data. To maintain consistency and clarity throughout the simulation study, we decide to keep the same GNN architecture across all sections of simulation study.

We then study the **square root** interference term, which indicates that the marginal benefit of allocating more treatments decreases constantly. This novel case also corresponds to a large category of scenarios. Specifically, the potential outcome model is:

$$Y_i(\mathbf{z}) = \beta_0 + \beta_1 z_i + \beta_2 \sqrt{\left(\frac{\sum_{j \in \mathcal{N}(i)} z_j}{\deg_i} \right)} + \epsilon_i \quad (46)$$

with the same parameters $(\beta_0, \beta_1, \beta_2, \sigma_e) = (1, 1, 1, 0.1)$. We present corresponding results in Table 13 and 14.

Table 13: The performance of GNN estimator with **square root** interference term

level metric rounds	Unit			Cluster		
	Bias	Std	MSE	Bias	Std	MSE
$t = 1$	-0.905	0.042	0.821	-0.623	0.051	0.391
$t = 2$	-0.387	0.014	0.150	-0.180	0.046	0.035
$t = 3$	-0.185	0.012	0.034	-0.063	0.052	0.007
$t = 4$	-0.086	0.010	0.008	0.021	0.057	0.004
$t = 5$	-0.006	0.012	0.000	0.030	0.081	0.007

Table 14: The performance of GNN estimator with **square root** interference term and merged data of $c_1 = 0$ and different c_t .

level metric proportion	Unit			Cluster		
	Bias	Std	MSE	Bias	Std	MSE
$c_t = 0.02$	-0.324	0.027	0.106	0.218	0.304	0.140
$c_t = 0.05$	-0.090	0.109	0.020	0.696	0.241	0.543
$c_t = 0.10$	0.519	0.050	0.272	0.895	0.145	0.822
$c_t = 0.25$	0.528	0.030	0.280	0.579	0.091	0.344
$c_t = 0.50$	0.218	0.008	0.048	0.250	0.057	0.066

We observe that cluster-level randomization is not necessary to achieve remarkable statistical performance. Moreover, the performance achieved by only merging 2-step becomes bad in the early stages of the ramp-up process.

We conclude that, from the perspective of one-dimensional function approximation¹³, additional data points help fit the nonlinear component more effectively. Therefore, when the interference term is nonlinear and is beyond our general interference setting, we recommend merging more experimental data from previous steps.

¹³As proposed in [20], the mean outcome under a specific randomization scheme with treatment proportion p can be viewed as a one-dimensional function of p .

5.5 Multihop interference

Moreover, we implement the **multihop** interference as shown in Example 2. Specifically, we maintain the setting that $(\beta_0, \beta_1, \beta_2, \sigma_e) = (1, 1, 1, 0.1)$, and set $M = 2$ and $(r_1, r_2) = (1, 0.5)$. Therefore, the true GATE in this case is given by:

$$\text{GATE} = (\beta_0 + \beta_1 + \frac{\beta_2}{n} \mathbf{1}^T B \mathbf{1}) - \beta_0 \approx 2.489 \quad (47)$$

The numerical outcome depends on the concrete network topology since we remove the circular effect that is introduced by the power of the (normalized) adjacency matrix. If we did not remove the diagonal terms of the interference matrix B , the GATE would be $\beta_1 + \beta_2(r_1 + r_2) = 2.5$. The results for our default setting are presented in Table 15. For completeness, we also include the results of training the regression model on merged 2-step experimental data with $c_1 = 0$ and varying c_t in Table 16.

Table 15: The performance of GNN estimator with **multihop** interference term

level metric rounds	Unit			Cluster		
	Bias	Std	MSE	Bias	Std	MSE
	$t = 1$	$t = 2$	$t = 3$	$t = 4$	$t = 5$	
	-1.401	0.034	1.963	-0.950	0.045	0.904
	-0.611	0.024	0.374	-0.303	0.064	0.096
	-0.316	0.013	0.100	-0.117	0.046	0.016
	-0.159	0.015	0.025	-0.061	0.064	0.008
	-0.160	0.024	0.026	-0.074	0.070	0.010

Table 16: The performance of GNN estimator with **multihop** interference term and merged data of $c_1 = 0$ and different c_t .

level metric proportion	Unit			Cluster		
	Bias	Std	MSE	Bias	Std	MSE
	$c_t = 0.02$	$c_t = 0.05$	$c_t = 0.10$	$c_t = 0.25$	$c_t = 0.50$	
	-0.977	0.032	0.956	-0.537	0.251	0.351
	-0.751	0.043	0.566	-0.217	0.159	0.072
	-0.580	0.078	0.342	-0.129	0.141	0.037
	-0.293	0.020	0.086	-0.094	0.061	0.012
	-0.183	0.012	0.033	-0.083	0.037	0.008

We first comment that the difference between 1-hop and multihop is intrinsic. For example, the HT estimator utilizes an exposure indicator that can provide an unbiased estimate when neighborhood interference assumption holds, despite the high variance. The form of this estimator is given by:

$$\hat{\tau}_{\text{exposure-HT}} = \frac{1}{n} \sum_{i \in [n]} \left(\left(\frac{\delta_i(1)}{\mathbb{E}[\delta_i(1)]} - \frac{\delta_i(0)}{\mathbb{E}[\delta_i(0)]} \right) Y_i(\mathbf{z}) \right) \quad (48)$$

Here, the indicator function δ_i is defined as $\delta_i(z_0) = \mathbb{I}\{\sum_{j \in \mathcal{N}_i} z_j / \deg_i = z_0\}$. However, when the interference goes beyond the 1-hop neighborhood, the estimation of $\mathbb{E}[\delta_i(z)]$ will incur computational

intractability if δ_i is adjusted to consider every unit's 2-hop neighborhood. On the other hand, if δ_i remains unchanged, the unbiasedness is lost, while the high variance remains.

Nonetheless, we observe that our methodology continues to support the GNN estimator in achieving remarkable statistical performance. In fact, the increase in the range of interference from 1-hop to 2-hop does not pose significant challenges to our methodology. We partially attribute this success to the power of graph convolution: with three convolution layers in our GNN model, the receptive field encompasses the 3-hop neighborhood of each node. This extensive receptive field helps maintain a low approximation error, even as the range of interference expands.

At last, we supplement that the standard HT estimator achieves bias -0.908 and standard deviation 0.563 , under cluster-level complete randomization with treatment proportion $c = 0.5$.

5.6 Dynamic Graph Structure

Finally, we consider the setting of a dynamic graph structure, which is novel in the literature but common in practice. For instance, if each experiment is conducted over a period of one week, the edges of the graph can change within that week, even in social networks. New friendships may form, and existing ones may be dissolved. The evolution of network structure is well-documented in network science, with models such as the Barabási-Albert Model [7] and the Forest Fire Model [43]. Although this aspect is still underexplored in the context of network experiments, it is valuable to consider this practical factor in sequential multiple experiments, such as in the ramp-up process.

Remark. Here, for simplicity, we consider the exogenous network evolution that is independent of treatment assignment. This is because the treatments typically considered by online platforms, such as new product features, generally do not have a significant impact on social relationships. However, there is existing literature in economics that examines cases where treatment does endogenously influence network formation, usually when the treatment itself has is more powerful.

For simplicity, we keep the node set unchanged throughout the ramp-up process and focus on modeling the addition of new edges over time. Inspired by classic preferential attachment, we generate edges for nodes with degrees in the top 50%. For each such node i , we connect it to node j with the following probability:

$$p_{ij} = \frac{\deg_j}{\sum_k \deg_k} \quad (49)$$

In each evolution, we repeat this sampling procedure 5 times with replacement for each node with degrees in the top 50%. If a unit i is sampled when generating edges for itself, we discard this sampling to avoid self-loops. Additionally, if the sampled unit j is already connected to unit i at the current step, we also discard this sampling to avoid creating multiple edges.

Given the ramp-up steps $(c_1, c_2, \dots, c_5) = (2\%, 5\%, 10\%, 25\%, 50\%)$, we take the initial network topology \mathcal{G} as baseline and repeat such evolution 5 times to generate evolved graphs with the same node set. The number of edges:

$$|\mathcal{E}_1|, \dots, |\mathcal{E}_5| = 596414, 624465, 652391, 680313, 708274 \quad (50)$$

where \mathcal{E}_t is the edge set at the t -th step.

Moreover, we go back to use the classic linear potential outcome in Example 1 and examine the influence of dynamic graph structure. The main parameter is set as $(\beta_0, \beta_1, \beta_2, \sigma_e) = (1, 1, 1, 0.1)$, as well as cases before. Even if the graph structure evolves, the GATE maintains to be $\beta_1 + \beta_2 = 2$. We present the result in Table 17 and 18.

Table 17: The performance of GNN estimator with **dynamic** graph structure.

level metric rounds	Unit			Cluster		
	Bias	Std	MSE	Bias	Std	MSE
$t = 1$	-0.666	0.095	0.453	-0.665	0.025	0.443
$t = 2$	-0.150	0.132	0.040	-0.161	0.061	0.030
$t = 3$	-0.106	0.137	0.030	-0.094	0.028	0.010
$t = 4$	-0.060	0.141	0.023	-0.058	0.044	0.005
$t = 5$	-0.045	0.149	0.024	-0.034	0.070	0.006

Table 18: The performance of GNN estimator with **dynamic** graph structure and merged data of $c_1 = 0$ and different c_t .

level metric proportion	Unit			Cluster		
	Bias	Std	MSE	Bias	Std	MSE
$c_t = 0.02$	-0.196	0.061	0.042	-0.220	0.135	0.067
$c_t = 0.05$	-0.069	0.048	0.007	-0.086	0.055	0.010
$c_t = 0.10$	-0.092	0.037	0.010	-0.084	0.041	0.009
$c_t = 0.25$	-0.107	0.021	0.012	-0.100	0.025	0.011
$c_t = 0.50$	-0.099	0.031	0.011	-0.098	0.028	0.010

The impact of evolutionary changes is quite complex, with classic models typically only characterizing the limiting behavior of preferential attachment. Nonetheless, our methodology consistently enhances the GNN model’s performance. During the evolution process, we preserve the clustering of the original topology \mathcal{G} to implement the staggered rollout design¹⁴, although this clustering may become less effective as edges are continuously added. As a result, our suggested practice of merging data with global control and the highest treatment proportion faces challenges due to the increasing discrepancy between \mathcal{G}_t and \mathcal{G} as step t progresses. This provides an intuitive explanation for why the monotonic improvement observed with increasing c_t , as shown in Table 7, no longer persists in Table 18. This reveals a potential limitation of this merging strategy in practice.

Remark. The rationale for generating edges solely for high-degree nodes stems from the distribution of treatment exposure, as detailed in Section 4. Low-degree nodes typically have exposure values concentrated at the boundaries of the interval $[0, 1]$, which significantly contributes to the variation in

¹⁴The time complexity of the Louvain algorithm supports weekly updates for clustering on large online platforms. However, when clustering changes, monotonic treatment assignment may no longer be guaranteed under cluster-level randomization.

exposures. To preserve this distinctive structure, we intentionally avoid generating new edges for all nodes. However, we do allow low-degree nodes to receive new edges initiated by high-degree nodes.

6 Discussion

In this paper, we propose a succinct and effective methodology of merging experimental data to unleash the potential of regression-based estimator, for the task of GATE estimation under network interference. The experimental data with different treatment proportions are a natural side product of the ramp-up process, demonstrating the practical applicability of our methodology: no additional experiments or specialized randomization schemes are required.

To develop our methodology, we examine the general linear interference model and a simple linear regression estimator, which together enable a detailed analysis of bias and variance when we merge the experimental data for model training. We first establish a series of theoretical results highlighting the significance of bias relative to variance in the context of regression-based estimators. Subsequently, we accurately characterize the substantial bias reduction achieved by merging experimental data with distinctly different treatment proportions.

To further illustrate the benefits of merging, we provide an intuitive perspective: merging increases the variation in treatment exposures. This intuition is grounded in statistical learning principles, as increased variation is essential for effective learning, and regression-based estimators involve a learning step. From this viewpoint, we also introduce a novel understanding of the role of cluster-level randomization, which partially highlights the synergistic effect of combining our methodology with cluster-level randomization, as demonstrated in our simulation study.

In the simulation study, we shift our focus to a more powerful and appropriate regression model, GNN. We begin by conducting an extensive setting to tease out the influential factors, and then analyze the results to verify that conclusions and insights derived from linear regression can also generalize to the GNN model. Next, we explore many challenging settings, including the multiplicative potential outcome model, linear potential outcome model with quadratic/square root interference term, multihop linear potential outcome model, and dynamic graph structure. The last three of them are novel in the simulation study of related works. Through these investigations, we demonstrate the impressive statistical performance achieved by our methodology.

To begin our discussion, we first highlight the dominant role of bias in this paper. In fact, the direct influence of interference is introducing bias. However, with the neighborhood interference assumption, which utilizes the exposure indicator (as shown in Equation (48)), can achieve unbiasedness easily. Such cases have received significant attention, emphasizing the variance reduction. Nevertheless, we argue that the primary challenge lies in addressing bias, particularly when network interference is widespread across the graph. In general, an unbiased estimator may be far from optimal in the presence of a bias-variance tradeoff. For instance, Hájek estimator introduces a slight bias but achieves significant bias reduction. A similar discussion is presented in the context of Markovian interference [23], where a biased estimator achieves a remarkable improvement in MSE compared to the unbiased estimator, with

the resulting variance being of a lower order than the bias, resembling our case.

We also note that when using the GNN estimator, conducting inference or constructing a valid confidence interval for our estimand, GATE, is quite challenging without strong structural assumptions that limit the form of interference. For instance, exposure mapping assumption [27, 45] is necessary for building CLT-type asymptotics. The latter paper also considers GNN model for observational data, and 1-hop exposure is utilized there for developing asymptotics. Recently, the technique of conformal prediction has been developed for implementing valid statistical inference in complex scenarios for a variety of black-box regression models, especially, network data [51] and GNN [35]. Despite the possible temporal dependency introduced by staggered rollout¹⁵, the main subtle point of our scenario lies in the GATE¹⁶—it is the average across all units in the finite population, while the confidence interval constructed through conformal prediction targets the individual sample. Hence, we leave statistical inference in our setting as future direction.

Furthermore, we do not take covariate (e.g. demographics) and the interaction term composed of covariate and treatment into the discussion of this paper, for theoretical convenience and better clarity. Nonetheless, it is worth noting that the GNN estimator can readily accommodate these elements by increasing the dimensionality of the input in the first layer.

Finally, we hope that our merging methodology will assist online platforms in achieving more precise and credible GATE estimations during the ramp-up process, which is crucial for the iterative development of products. We also expect that this work will draw further attention from researchers to the regression-based estimator, which, as demonstrated in this paper, proves to be a powerful tool for causal inference in the presence of complex interference.

¹⁵There are also techniques of conformal prediction developed to tackle the situation where exchangeability is violated [8], specifically, temporal dependency among features.

¹⁶Based on exposure mapping assumption, the estimand usually changes to the difference between the mean outcome under two different exposure conditions. In this case, there exists repetitions of units in the population to support CLT.

References

- [1] Anish Agarwal, Sarah H. Cen, Devavrat Shah, and Christina Lee Yu. Network synthetic interventions: A causal framework for panel data under network interference, 2023.
- [2] Peter M Aronow and Cyrus Samii. Estimating average causal effects under general interference, with application to a social network experiment. *Annals of Applied Statistics*, 11(4):1912–1947, 2017.
- [3] Susan Athey, Mohsen Bayati, Nikolay Doudchenko, Guido Imbens, and Khashayar Khosravi. Matrix completion methods for causal panel data models. *Journal of the American Statistical Association*, 116(536):1716–1730, 2021.
- [4] Susan Athey, Dean Eckles, and Guido W Imbens. Exact p-values for network interference. *Journal of the American Statistical Association*, 113(521):230–240, 2018.
- [5] Sarah Baird, J Aislinn Bohren, Craig McIntosh, and Berk Özler. Optimal design of experiments in the presence of interference. *Review of Economics and Statistics*, 100(5):844–860, 2018.
- [6] Patrick Bajari, Brian Burdick, Guido W Imbens, Lorenzo Masoero, James McQueen, Thomas S Richardson, and Ido M Rosen. Experimental design in marketplaces. *Statistical Science*, 38(3):458–476, 2023.
- [7] Albert-László Barabási and Réka Albert. Emergence of scaling in random networks. *science*, 286(5439):509–512, 1999.
- [8] Rina Foygel Barber, Emmanuel J Candes, Aaditya Ramdas, and Ryan J Tibshirani. Conformal prediction beyond exchangeability. *The Annals of Statistics*, 51(2):816–845, 2023.
- [9] Guillaume W Basse and Edoardo M Airoldi. Model-assisted design of experiments in the presence of network-correlated outcomes. *Biometrika*, 105(4):849–858, 2018.
- [10] Rohit Bhattacharya, Daniel Malinsky, and Ilya Shpitser. Causal inference under interference and network uncertainty. In *Uncertainty in Artificial Intelligence*, pages 1028–1038. PMLR, 2020.
- [11] Vincent D Blondel, Jean-Loup Guillaume, Renaud Lambiotte, and Etienne Lefebvre. Fast unfolding of communities in large networks. *Journal of statistical mechanics: theory and experiment*, 2008(10):P10008, 2008.
- [12] Iavor Bojinov, David Simchi-Levi, and Jinglong Zhao. Design and analysis of switchback experiments. *Management Science*, 69(7):3759–3777, 2023.
- [13] Ariel Boyarsky, Hongseok Namkoong, and Jean Pouget-Abadie. Modeling interference using experiment roll-out. In Kevin Leyton-Brown, Jason D. Hartline, and Larry Samuelson, editors, *Proceedings of the 24th ACM Conference on Economics and Computation, EC 2023, London, United Kingdom, July 9-12, 2023*, page 298. ACM, 2023.

- [14] Jennifer Brennan, Vahab Mirrokni, and Jean Pouget-Abadie. Cluster randomized designs for one-sided bipartite experiments. *Advances in Neural Information Processing Systems*, 35:37962–37974, 2022.
- [15] Ido Bright, Arthur Delarue, and Ilan Lobel. Reducing marketplace interference bias via shadow prices. *arXiv preprint arXiv:2205.02274*, 2022.
- [16] Chencheng Cai, Xu Zhang, and Edoardo Airoldi. Independent-set design of experiments for estimating treatment and spillover effects under network interference. In *The Twelfth International Conference on Learning Representations*, 2024.
- [17] Ozan Candogan, Chen Chen, and Rad Niazadeh. Correlated cluster-based randomized experiments: Robust variance minimization. *Management Science*, 2023.
- [18] Qianyi Chen, Bo Li, Lu Deng, and Yong Wang. Optimized covariance design for ab test on social network under interference. *Advances in Neural Information Processing Systems*, 36, 2024.
- [19] Weilin Chen, Ruichu Cai, Zequin Yang, Jie Qiao, Yuguang Yan, Zijian Li, and Zhifeng Hao. Doubly robust causal effect estimation under networked interference via targeted learning. In *Forty-first International Conference on Machine Learning*, 2024.
- [20] Mayleen Cortez, Matthew Eichhorn, and Christina Yu. Staggered rollout designs enable causal inference under interference without network knowledge. In *Advances in Neural Information Processing Systems*, 2022.
- [21] Michaël Defferrard, Xavier Bresson, and Pierre Vandergheynst. Convolutional neural networks on graphs with fast localized spectral filtering. *Advances in neural information processing systems*, 29, 2016.
- [22] Dean Eckles, Brian Karrer, and Johan Ugander. Design and analysis of experiments in networks: Reducing bias from interference. *Journal of Causal Inference*, 5(1):20150021, 2016.
- [23] Vivek Farias, Andrew Li, Tianyi Peng, and Andrew Zheng. Markovian interference in experiments. *Advances in Neural Information Processing Systems*, 35:535–549, 2022.
- [24] Vivek Farias, Hao Li, Tianyi Peng, Xinyuyang Ren, Huawei Zhang, and Andrew Zheng. Correcting for interference in experiments: A case study at douyin. In *Proceedings of the 17th ACM Conference on Recommender Systems*, pages 455–466, 2023.
- [25] Laura Forastiere, Edoardo M Airoldi, and Fabrizia Mealli. Identification and estimation of treatment and interference effects in observational studies on networks. *Journal of the American Statistical Association*, 116(534):901–918, 2021.
- [26] Laura Forastiere, Fabrizia Mealli, Albert Wu, and Edoardo M Airoldi. Estimating causal effects under network interference with bayesian generalized propensity scores. *Journal of Machine Learning Research*, 23(289):1–61, 2022.

- [27] Mengsi Gao and Peng Ding. Causal inference in network experiments: regression-based analysis and design-based properties. *arXiv preprint arXiv:2309.07476*, 2023.
- [28] Peter W Glynn, Ramesh Johari, and Mohammad Rasouli. Adaptive experimental design with temporal interference: A maximum likelihood approach. *Advances in Neural Information Processing Systems*, 33:15054–15064, 2020.
- [29] Ali Goli, Anja Lambrecht, and Hema Yoganarasimhan. A bias correction approach for interference in ranking experiments. *Marketing Science*, 43(3):590–614, 2024.
- [30] Huan Gui, Ya Xu, Anmol Bhasin, and Jiawei Han. Network a/b testing: From sampling to estimation. In *24th International Conference on World Wide Web, WWW 2015*, pages 399–409. Association for Computing Machinery, Inc, 2015.
- [31] Kevin Han, Shuangning Li, Jialiang Mao, and Han Wu. Detecting interference in online controlled experiments with increasing allocation. In *Proceedings of the 29th ACM SIGKDD Conference on Knowledge Discovery and Data Mining*, pages 661–672, 2023.
- [32] Kevin Han and Johan Ugander. Model-based regression adjustment with model-free covariates for network interference. *Journal of Causal Inference*, 11(1):20230005, 2023.
- [33] Christopher Harshaw, Fredrik Sävje, David Eisenstat, Vahab Mirrokni, and Jean Pouget-Abadie. Design and analysis of bipartite experiments under a linear exposure-response model. *Electronic Journal of Statistics*, 17(1):464–518, 2023.
- [34] David Holtz, Felipe Lobel, Ruben Lobel, Inessa Liskovich, and Sinan Aral. Reducing interference bias in online marketplace experiments using cluster randomization: Evidence from a pricing meta-experiment on airbnb. *Management Science*, 2024.
- [35] Kexin Huang, Ying Jin, Emmanuel Candes, and Jure Leskovec. Uncertainty quantification over graph with conformalized graph neural networks. *Advances in Neural Information Processing Systems*, 36, 2024.
- [36] Michael G Hudgens and M Elizabeth Halloran. Toward causal inference with interference. *Journal of the American Statistical Association*, 103(482):832–842, 2008.
- [37] Yiming Jiang and He Wang. Causal inference under network interference using a mixture of randomized experiments. *arXiv preprint arXiv:2309.00141*, 2023.
- [38] Ramesh Johari, Hannah Li, Inessa Liskovich, and Gabriel Y Weintraub. Experimental design in two-sided platforms: An analysis of bias. *Management Science*, 68(10):7069–7089, 2022.
- [39] Tay Kenneth and Wang Xiaofeng. Ocelot: Scaling observational causal inference at linkedin, 2022.
- [40] Diederik P Kingma and Jimmy Ba. Adam: A method for stochastic optimization. *arXiv preprint arXiv:1412.6980*, 2014.
- [41] Ron Kohavi, Roger Longbotham, Dan Sommerfield, and Randal M Henne. Controlled experiments on the web: survey and practical guide. *Data mining and knowledge discovery*, 18:140–181, 2009.

- [42] Ron Kohavi, Diane Tang, and Ya Xu. *Trustworthy online controlled experiments: A practical guide to a/b testing*. Cambridge University Press, 2020.
- [43] Jure Leskovec, Jon Kleinberg, and Christos Faloutsos. Graphs over time: densification laws, shrinking diameters and possible explanations. In *Proceedings of the eleventh ACM SIGKDD international conference on Knowledge discovery in data mining*, pages 177–187, 2005.
- [44] Michael P Leung. Rate-optimal cluster-randomized designs for spatial interference. *The Annals of Statistics*, 50(5):3064–3087, 2022.
- [45] Michael P. Leung and Pantelis Loupos. Graph neural networks for causal inference under network confounding, 2024.
- [46] Hannah Li, Geng Zhao, Ramesh Johari, and Gabriel Y Weintraub. Interference, bias, and variance in two-sided marketplace experimentation: Guidance for platforms. In *Proceedings of the ACM Web Conference 2022*, pages 182–192, 2022.
- [47] Shuangning Li and Stefan Wager. Random graph asymptotics for treatment effect estimation under network interference. *The Annals of Statistics*, 50(4):2334–2358, 2022.
- [48] Lan Liu, Michael G Hudgens, and Sylvia Becker-Dreps. On inverse probability-weighted estimators in the presence of interference. *Biometrika*, 103(4):829–842, 2016.
- [49] Yang Liu, Yifan Zhou, Ping Li, and Feifang Hu. Adaptive a/b test on networks with cluster structures. In *International Conference on Artificial Intelligence and Statistics*, pages 10836–10851. PMLR, 2022.
- [50] Yang Liu, Yifan Zhou, Ping Li, and Feifang Hu. Cluster-adaptive network a/b testing: From randomization to estimation. *Journal of Machine Learning Research*, 25(170):1–48, 2024.
- [51] Robert Lunde, Elizaveta Levina, and Ji Zhu. Conformal prediction for network-assisted regression. *arXiv preprint arXiv:2302.10095*, 2023.
- [52] Jialiang Mao and Iavor Bojinov. Quantifying the value of iterative experimentation. *arXiv preprint arXiv:2111.02334*, 2021.
- [53] Tu Ni, Iavor Bojinov, and Jinglong Zhao. Design of panel experiments with spatial and temporal interference. *Available at SSRN 4466598*, 2023.
- [54] Ben M Parker, Steven G Gilmour, and John Schormans. Optimal design of experiments on connected units with application to social networks. *Journal of the Royal Statistical Society. Series C (Applied Statistics)*, pages 455–480, 2017.
- [55] Jean Pouget-Abadie, Kevin Aydin, Warren Schudy, Kay Brodersen, and Vahab Mirrokni. Variance reduction in bipartite experiments through correlation clustering. *Advances in Neural Information Processing Systems*, 32, 2019.

- [56] Jean Pouget-Abadie, Guillaume Saint-Jacques, Martin Saveski, Weitao Duan, Souvik Ghosh, Ya Xu, and Edoardo M Airoldi. Testing for arbitrary interference on experimentation platforms. *Biometrika*, 106(4):929–940, 2019.
- [57] Paul R Rosenbaum. Interference between units in randomized experiments. *Journal of the american statistical association*, 102(477):191–200, 2007.
- [58] Ryan A. Rossi and Nesreen K. Ahmed. The network data repository with interactive graph analytics and visualization. In *AAAI*, 2015.
- [59] Donald B Rubin. Estimating causal effects of treatments in randomized and nonrandomized studies. *Journal of educational Psychology*, 66(5):688, 1974.
- [60] Fredrik Sävje. Causal inference with misspecified exposure mappings: separating definitions and assumptions. *Biometrika*, 111(1):1–15, 2024.
- [61] Sadegh Shirani and Mohsen Bayati. Causal message-passing for experiments with unknown and general network interference. *Proceedings of the National Academy of Sciences*, 121(40):e2322232121, 2024.
- [62] Michael E Sobel. What do randomized studies of housing mobility demonstrate? causal inference in the face of interference. *Journal of the American Statistical Association*, 101(476):1398–1407, 2006.
- [63] Vydhourie Thiyyageswaran, Tyler McCormick, and Jennifer Brennan. Data-adaptive exposure thresholds for the horvitz-thompson estimator of the average treatment effect in experiments with network interference. *arXiv preprint arXiv:2405.15887*, 2024.
- [64] Johan Ugander, Brian Karrer, Lars Backstrom, and Jon Kleinberg. Graph cluster randomization: Network exposure to multiple universes. In *Proceedings of the 19th ACM SIGKDD international conference on Knowledge discovery and data mining*, pages 329–337, 2013.
- [65] Johan Ugander and Hao Yin. Randomized graph cluster randomization. *Journal of Causal Inference*, 11(1):20220014, 2023.
- [66] Gonzalo Vazquez-Bare. Identification and estimation of spillover effects in randomized experiments. *Journal of Econometrics*, 237(1):105237, 2023.
- [67] Davide Viviano. Experimental design under network interference, 2022.
- [68] Davide Viviano, Lihua Lei, Guido Imbens, Brian Karrer, Okke Schrijvers, and Liang Shi. Causal clustering: design of cluster experiments under network interference, 2024.
- [69] Stefan Wager and Kuang Xu. Experimenting in equilibrium. *Management Science*, 67(11):6694–6715, 2021.
- [70] Caio Waisman, Navdeep S Sahni, Harikesh S Nair, and Xiliang Lin. Parallel experimentation and competitive interference on online advertising platforms. *Marketing Science*, 2024.

- [71] Runzhe Wan, Yu Liu, James McQueen, Doug Hains, and Rui Song. Experimentation platforms meet reinforcement learning: Bayesian sequential decision-making for continuous monitoring. In *Proceedings of the 29th ACM SIGKDD Conference on Knowledge Discovery and Data Mining*, pages 5016–5027, 2023.
- [72] Minjie Wang, Da Zheng, Zihao Ye, Quan Gan, Mufei Li, Xiang Song, Jinjing Zhou, Chao Ma, Lingfan Yu, Yu Gai, Tianjun Xiao, Tong He, George Karypis, Jinyang Li, and Zheng Zhang. Deep graph library: A graph-centric, highly-performant package for graph neural networks. *arXiv preprint arXiv:1909.01315*, 2019.
- [73] Ruoxuan Xiong, Susan Athey, Mohsen Bayati, and Guido Imbens. Optimal experimental design for staggered rollouts. *Management Science*, 2023.
- [74] Ya Xu, Weitao Duan, and Shaochen Huang. Sqr: Balancing speed, quality and risk in online experiments. In *Proceedings of the 24th ACM SIGKDD International Conference on Knowledge Discovery & Data Mining*, pages 895–904, 2018.
- [75] Christina Lee Yu, Edoardo M Airoldi, Christian Borgs, and Jennifer T Chayes. Estimating the total treatment effect in randomized experiments with unknown network structure. *Proceedings of the National Academy of Sciences*, 119(44):e2208975119, 2022.
- [76] Yuan Yuan and Kristen M. Altenburger. A two-part machine learning approach to characterizing network interference in a/b testing, 2024.
- [77] Corwin M Zigler and Georgia Papadogeorgou. Bipartite causal inference with interference. *Statistical science: a review journal of the Institute of Mathematical Statistics*, 36(1):109, 2021.

A Proofs

A.1 Proof of Theorem 1

Proof. First, our simple linear regression estimator gives:

$$\hat{\tau} = (\hat{\theta}_1 + \hat{\theta}_0) - \hat{\theta}_0 = \hat{\theta}_1 \quad (51)$$

and

$$\hat{\theta} = (X(\mathbf{z})^T X(\mathbf{z}))^{-1} X(\mathbf{z})^T Y \quad (52)$$

For the simplicity in the derivation, we write $X = X(\mathbf{z})$ in the following. Since we consider complete randomization, there are n units and we assign d treatments exactly. We have:

$$X^T X = \begin{pmatrix} n & \mathbf{z}^T \mathbf{1} \\ \mathbf{z}^T \mathbf{1} & \|\mathbf{z}\|_2^2 \end{pmatrix} = \begin{pmatrix} n & d \\ d & d \end{pmatrix} \quad (53)$$

and

$$(X^T X)^{-1} X^T = \frac{1}{d(n-d)} \begin{pmatrix} d(\mathbf{1} - \mathbf{z})^T \\ (n\mathbf{z} - d\mathbf{1})^T \end{pmatrix} \quad (54)$$

Notice that Y can be written as

$$Y = \begin{pmatrix} X & B\mathbf{z} \end{pmatrix} \beta \quad (55)$$

Here, the shape of X is $n \times 2$, $B\mathbf{z}$ is $n \times 1$, and β is 3×1 .

The expression of $\hat{\theta}$ is given by

$$\begin{aligned} \hat{\theta} &= (X^T X)^{-1} X^T Y \\ &= \begin{pmatrix} I_2 & (X^T X)^{-1} X^T B\mathbf{z} \end{pmatrix} \beta + (X^T X)^{-1} X^T \epsilon \\ &= \left(I_2 - \frac{1}{d(n-d)} \begin{pmatrix} d(\mathbf{1} - \mathbf{z})^T B\mathbf{z} \\ (n\mathbf{z} - d\mathbf{1})^T B\mathbf{z} \end{pmatrix} \right) + (X^T X)^{-1} X^T \epsilon \end{aligned} \quad (56)$$

Since we're only concerned with $\hat{\theta}_1$, we directly take the second term of $\hat{\theta}$:

$$\hat{\theta}_1 = \beta_1 + \beta_2 \frac{1}{d(n-d)} (n\mathbf{z} - d\mathbf{1})^T B\mathbf{z} + \frac{1}{d(n-d)} (n\mathbf{z} - d\mathbf{1})^T \epsilon \quad (57)$$

Notice that $\mathbf{z} \perp \epsilon$. The **bias** is given by

$$\mathbb{E}[\hat{\theta}_1] - (\beta_1 + \beta_2 \frac{1}{n} \text{trace}(\mathbf{1}\mathbf{1}^T B)) = \frac{\beta_2}{nc(1-c)} \mathbb{E}[(\mathbf{z} - c\mathbf{1})^T B\mathbf{z}] - \frac{\beta_2}{n} \text{trace}(\mathbf{1}\mathbf{1}^T B) \quad (58)$$

Next, we evaluate the term $\mathbb{E}[(\mathbf{z} - c\mathbf{1})^T B\mathbf{z}]$, which is given by:

$$\begin{aligned}
\mathbb{E}[(\mathbf{z} - c\mathbf{1})^T B\mathbf{z}] &= \mathbb{E}[\text{trace}((\mathbf{z} - c\mathbf{1})^T B\mathbf{z})] \\
&= \mathbb{E}[\text{trace}(\mathbf{z}(\mathbf{z} - c\mathbf{1})^T B)] \\
&= \text{trace}(\mathbb{E}[\mathbf{z}(\mathbf{z} - c\mathbf{1})^T] B) \\
&= \text{trace}\left((c\frac{d-1}{n-1} - c^2)\mathbf{1}\mathbf{1}^T B\right) \\
&= -\frac{c(1-c)}{n-1} \text{trace}(\mathbf{1}\mathbf{1}^T B)
\end{aligned} \tag{59}$$

Plugging it into the expression of bias, we get:

$$\text{Bias} = -\frac{\beta_2}{n} \left(\sum_{i,j} B_{ij} \right) \left(\frac{1}{n(n-1)} + 1 \right) \tag{60}$$

Subsequently, we derive the expression of variance. Noting that $\mathbf{z} \perp \epsilon$ and $\mathbb{E}[\epsilon] = \mathbf{0}$, we have:

$$\text{Cov}[(n\mathbf{z} - d\mathbf{1})^T B\mathbf{z}, (n\mathbf{z} - d\mathbf{1})^T \epsilon] = 0 \tag{61}$$

Thus, we can omit all the covariance terms in the expression of variance, yielding:

$$\text{Var}(\hat{\tau}) = \left(\frac{\beta_2}{nc(1-c)} \right)^2 \text{Var}((\mathbf{z} - c\mathbf{1})^T B\mathbf{z}) + \frac{1}{(nc(1-c))^2} \mathbb{E}[(\mathbf{z} - c\mathbf{1})^T (\mathbf{z} - c\mathbf{1})] \sigma_e^2 \tag{62}$$

First, we consider the second term above, which represents the variance induced by ϵ :

$$\begin{aligned}
\text{Var}_e &= \frac{1}{(d(n-d))^2} \mathbb{E}[(n\mathbf{z} - d\mathbf{1})^T (n\mathbf{z} - d\mathbf{1})] \sigma_e^2 \\
&= \left(\frac{n}{d(n-d)} \right)^2 \mathbb{E}[(\mathbf{z} - \frac{d}{n}\mathbf{1})^T (\mathbf{z} - \frac{d}{n}\mathbf{1})] \sigma_e^2 \\
&= \left(\frac{n\sigma_e}{d(n-d)} \right)^2 \mathbb{E}[d - \frac{2d}{n} \times d + \frac{d^2}{n}] \\
&= \left(\frac{n\sigma_e}{d(n-d)} \right)^2 (d - \frac{d^2}{n}) \\
&= \frac{\sigma_e^2}{nc(1-c)}
\end{aligned} \tag{63}$$

Next, we discuss the first term:

$$\left(\frac{\beta_2}{nc(1-c)} \right)^2 \text{Var}((\mathbf{z} - c\mathbf{1})^T B\mathbf{z}) \tag{64}$$

We use the expansion $\text{Var}(X) = \mathbb{E}[X^2] - E[X]^2$, and the square of expectation term has been simplified in equation (59). Thus, our focus is the expectation of square term, which can be expanded with

brute-force:

$$\left(\frac{\beta_2}{c(1-c)n}\right)^2 \sum_{i,j,k,l} B_{ij} B_{kl} \mathbb{E}[(z_i - c)(z_k - c)z_j z_l] \quad (65)$$

As mentioned in the main paper, our technique involves classifying the index set $I \subset [n]^4$ that restricts the quadruples (i, j, k, l) and calculating $\mathbb{E}[(z_i - c)(z_k - c)z_j z_l]$ respectively. Since $B_{ii} = 0$ for all $i \in [n]$, we do not need to consider the cases where $i = j$ or $k = l$. We present the result as follows:

1. $i = k, j = l, i \neq k$,

$$\begin{aligned} \mathbb{E}[(z_i - c)(z_k - c)z_j z_l] &= \mathbb{E}[(z_i - c)^2 z_j^2] \\ &= \mathbb{E}[(z_i - 2cz_i + c^2)z_j] \\ &= (1 - 2c)\mathbb{E}[z_i z_j] + c^2 \mathbb{E}[z_j] \\ &= (1 - 2c)c \frac{d-1}{n-1} + c^3 \\ &= \Theta(1) \end{aligned} \quad (66)$$

2. $i = l, k = j, i \neq k$

$$\begin{aligned} \mathbb{E}[(z_i - c)(z_k - c)z_j z_l] &= \mathbb{E}[(z_i - c)(z_k - c)z_i z_k] \\ &= \mathbb{E}[(1 - c)^2 z_i z_k] \\ &= (1 - c)^2 c \frac{d-1}{n-1} \\ &= \Theta(1) \end{aligned} \quad (67)$$

3. Only $i = k$ holds, with i, j , and l being distinct.

$$\begin{aligned} \mathbb{E}[(z_i - c)(z_k - c)z_j z_l] &= \mathbb{E}[(z_i - c)^2 z_k z_l] \\ &= (1 - 2c)\mathbb{E}[z_i z_k z_l] + c^2 \mathbb{E}[z_k z_l] \\ &= (1 - 2c)c \frac{(d-1)(d-2)}{(n-1)(n-2)} + c^3 \frac{d-1}{n-1} \\ &= \Theta(1) \end{aligned} \quad (68)$$

4. Only $j = l$ holds, with i, j , and k being distinct.

$$\begin{aligned} \mathbb{E}[(z_i - c)(z_k - c)z_j z_l] &= \mathbb{E}[(z_i - c)(z_k - c)z_j] \\ &= \frac{nd(d-n) + 2d^2 + 2n^2 - 4nd}{n^2(n-1)(n-2)} \\ &= \frac{c(d-n) + 2c^2 + 2 - 4c}{(n-1)(n-2)} \\ &= \Theta\left(\frac{1}{n}\right) \end{aligned} \quad (69)$$

5. i, j, k, l are all distinct.

$$\begin{aligned}
& \mathbb{E}[(z_i - c)(z_k - c)z_j z_l] \\
&= \mathbb{E}[(z_i z_k - c(z_i + z_k) + c^2)z_j z_l] \\
&= \frac{d(d-1)(d-2)(d-3)}{n(n-1)(n-2)(n-3)} - 2c \frac{d(d-1)(d-2)}{n(n-1)(n-2)} + c^2 \frac{d(d-1)}{n(n-1)} \\
&= \frac{d(d-1)}{n(n-1)} \left(\frac{(d-2)(d-3)}{(n-2)(n-3)} + \frac{d^2}{n^2} - 2 \frac{d(d-2)}{n(n-2)} \right) \\
&= \frac{d(d-1)}{n(n-1)} \left(\frac{(d^2 - 5d + 6)n^2 + d^2(n^2 - 5d + 6) - 2dn(dn - 2n - 3d + 6)}{n^2(n-2)(n-3)} \right) \quad (70) \\
&= \frac{d(d-1)}{n(n-1)} \left(\frac{(d^2 - 5d + 6)n^2 + d^2(n^2 - 5d + 6) - 2dn(dn - 2n - 3d + 6)}{n^2(n-2)(n-3)} \right) \\
&= \frac{c(d-1)}{(n-1)} \left(\frac{c(d-n) + 6 + 6c^2 - 12c}{(n-2)(n-3)} \right) \\
&= \Theta\left(\frac{1}{n}\right)
\end{aligned}$$

Combine these five cases and corresponding index sets, we get the expression of variance as presented in Theorem 1. For the convenience of proof of Corollary 1 later, we also annotate the order of each term at last line.

A.2 Proof of Corollary 1

Proof. Since Assumption 1 restricts

$$\sum_{i,j} B_{ij} = \Theta(n) \quad (71)$$

We get the order of bias instantly:

$$\text{Bias} = -\frac{\beta_2}{n} \left(\sum_{i,j} B_{ij} \right) \left(\frac{1}{n(n-1)} + 1 \right) = \Theta(1) \quad (72)$$

Next, we discuss the order of variance. It concerns bounding the order of the summations over five index sets mentioned in Appendix A.1. To begin with, we notice that the variance is non-negative and the variance induced by ϵ is:

$$\frac{\sigma_e^2}{\beta_2^2 n c (1-c)} = \Theta\left(\frac{1}{n}\right) \quad (73)$$

Thus, we can first claim that

$$\text{Var}(\hat{\tau}) = \Omega\left(\frac{1}{n}\right) \quad (74)$$

We then prove the first term in the expression of variance has a order of $O(1/n)$. Specifically, we bound those five summations respectively. According to the Assumption 1, we get a naive bound that will be

used repeatedly:

$$|B_{ij}| \leq \sum_j |B_{ij}| \leq b \quad (75)$$

1. $i = k, j = l, i \neq k$.

$$\sum_{ij} B_{ij}^2 \leq \sum_i b \sum_j |B_{ij}| \leq b^2 n \quad (76)$$

Thus,

$$\sum_{ij} B_{ij}^2 = O(n) \quad (77)$$

2. $i = l, k = j, i \neq k$

$$|\sum_{i,j} B_{ij} B_{ji}| \leq \sum_{i,j} |B_{ij} B_{ji}| \leq b \sum_{i,j} |B_{ij}| \leq b^2 n \quad (78)$$

Thus,

$$\sum_{ij} B_{ij} B_{ji} = O(n) \quad (79)$$

3. Only $i = k$ holds, with i, j , and l being distinct.

$$|\sum_{i,j,l} B_{ij} B_{il}| \leq \sum_{i,j,l} |B_{ij} B_{il}| = \sum_{i,j} |B_{ij}| \sum_l |B_{il}| \leq b \sum_{i,j} |B_{ij}| \leq b^2 n \quad (80)$$

Thus,

$$\sum_{i,j,l} B_{ij} B_{il} = O(n) \quad (81)$$

4. Only $j = l$ holds, with i, j , and k being distinct.

$$|\sum_{i,j,k} B_{ij} B_{kj}| \leq \sum_{i,j,k} |B_{ij} B_{kj}| \leq b \sum_{i,j,k} |B_{ij}| \leq b^2 n^2 \quad (82)$$

Thus,

$$\sum_{i,j,k} B_{ij} B_{kj} = O(n^2) \quad (83)$$

5. i, j, k, l are all distinct.

$$\sum_{i,j,k,l} B_{ij} B_{kl} = (\sum_{ij} B_{ij})^2 = \Theta(n^2) \quad (84)$$

Combine the orders of five summations above and the order of corresponding $\mathbb{E}[(z_i - c)(z_k - c)z_j z_l]$, we get:

$$\text{Var}(\hat{\tau}) = \Theta(\frac{1}{n}) \quad (85)$$

Finally, we comment that the bound on $|\sum_{i,j,k} B_{ij} B_{kj}|$ is rough, while we don't apply the third part of Assumption 1, i.e. restricting the order $\sum_{i,j,k} B_{ij} B_{kj} = \sum_j (\sum_i B_{ij})^2$ directly.

Such a rough bound is still acceptable because of the equation (69), i.e.

$$\mathbb{E}[(z_i - c)(z_k - c)z_j z_l] = \Theta\left(\frac{1}{n}\right) \quad (86)$$

For the situation of merging $T \geq 2$ experimental data, we will have:

$$\mathbb{E}[(z_i - \frac{\sum_{t=1}^T c_t}{T})(z_k - \frac{\sum_{t=1}^T c_t}{T})z_j z_l] = \Theta(1) \quad (87)$$

if $\frac{\sum_{t=1}^T c_t}{T} \neq \mathbb{E}[z_i]$. that is why we need further assumption to control the order variance there.

A.3 Proof of Theorem 2

Proof. In the situation of $T = 2$, the sample size increases from n to $2n$, and the number of treated units changes from d to $d_1 + d_2$. Correspondingly, the treatment proportions in two experiments are c_1 and c_2 . In linear regression, this additionally leads to the following two changes:

$$B \xrightarrow{\text{expand}} \begin{pmatrix} B & 0 \\ 0 & B \end{pmatrix} \quad \mathbf{z} \xrightarrow{\text{expand}} \begin{pmatrix} \mathbf{z}_1 \\ \mathbf{z}_2 \end{pmatrix} \quad (88)$$

We make the changes above and get

$$\begin{aligned} & \text{Bias}/(\beta_2 \sum_{i,j} B_{ij}) + 1 \\ &= \frac{2n}{(d_1 + d_2)(2n - (d_1 + d_2))} \text{trace} \left(\mathbb{E} \left[\mathbf{z}(\mathbf{z} - \frac{d_1 + d_2}{2n} \mathbf{1})^T \right] \begin{pmatrix} B & 0 \\ 0 & B \end{pmatrix} \right) \\ &= \frac{2n}{(d_1 + d_2)(2n - (d_1 + d_2))} \text{trace} \left(\left(\mathbb{E} [\mathbf{z}\mathbf{z}^T] - \frac{d_1 + d_2}{2n} \mathbb{E} [\mathbf{z}\mathbf{1}^T] \right) \begin{pmatrix} B & 0 \\ 0 & B \end{pmatrix} \right) \\ &= \frac{2n}{(d_1 + d_2)(2n - (d_1 + d_2))} \left(\text{trace} ((\mathbb{E}[\mathbf{z}_1\mathbf{z}_1^T] + \mathbb{E}[\mathbf{z}_2\mathbf{z}_2^T])B) - \frac{d_1 + d_2}{2n} \left(\frac{d_1}{n} + \frac{d_2}{n} \right) \text{trace} (\mathbf{1}\mathbf{1}^T B) \right) \\ &= \frac{2n}{(d_1 + d_2)(2n - (d_1 + d_2))} \left(\frac{d_1(d_1 - 1) + d_2(d_2 - 1)}{n(n-1)} - \frac{(d_1 + d_2)^2}{2n^2} \right) \text{trace} (\mathbf{1}\mathbf{1}^T B) \\ &= \frac{2n^2}{(d_1 + d_2)(2n - (d_1 + d_2))} \frac{(n-1)(d_1 - d_2)^2 + 2(d_1^2 + d_2^2) - 2n(d_1 + d_2)}{2n^2(n-1)} \\ &= \frac{(n-1)(d_1 - d_2)^2 + 2(d_1^2 + d_2^2) - 2n(d_1 + d_2)}{(n-1)(d_1 + d_2)(2n - (d_1 + d_2))} \\ &= \frac{(n-1)(c_1 - c_2)^2 + 2(c_1^2 + c_2^2) - 2(c_1 + c_2)}{(n-1)(c_1 + c_2)(2 - (c_1 + c_2))} \end{aligned} \quad (89)$$

Thus, we get:

$$\text{Bias}(\hat{\tau})/\beta_2 = -\frac{\sum_{ij} B_{ij}}{n} \left(1 - \frac{(n-1)(c_1 - c_2)^2 + 2(c_1^2 + c_2^2) - 2(c_1 + c_2)}{(n-1)(c_1 + c_2)(2 - (c_1 + c_2))} \right) \quad (90)$$

A.4 Proof of Theorem 3

Proof. As mentioned in the main paper, there is no additional challenge in deriving the result of $T > 2$ case. Refer to the fourth equation in equation (89), we now have:

$$\begin{aligned} \text{Bias}/(\beta_2 \sum_{i,j} B_{ij}) + 1 &= \frac{Tn}{\sum_{t=1}^T d_t (Tn - \sum_{t=1}^T d_t)} \left(\frac{\sum_{t=1}^T d_t (d_t - 1)}{n(n-1)} - \frac{(\sum_{t=1}^T d_t)^2}{Tn^2} \right) \\ &= \frac{T}{n(\sum_{t=1}^T c_t)(T - \sum_{t=1}^T c_t)} \left(\frac{T \sum_{t=1}^T c_t^2 - (\sum_{t=1}^T c_t)^2}{T} + O\left(\frac{1}{n}\right) \right) \end{aligned} \quad (91)$$

Thus, since $\sum_{i,j} B_{ij} = \Theta(n)$, we have:

$$\text{Bias}(\hat{\tau})/\beta_2 = -\frac{\sum_{i,j} B_{ij}}{n} \left(1 - \frac{T \sum_{t=1}^T c_t^2 - (\sum_{t=1}^T c_t)^2}{(\sum_{t=1}^T c_t)(T - \sum_{t=1}^T c_t)} \right) + O\left(\frac{1}{n}\right) \quad (92)$$

A.5 Proof of Corollary 2

Proof. We continue to use the notation in the main paper, and further bias reduction corresponds to:

$$\frac{kC_2 - C_1^2}{C_1(k - C_1)} < \frac{(k+1)(C_2 + x^2) - (C_1 + x)^2}{(C_1 + x)(k+1 - C_1 - x)} \quad (93)$$

We expand the two sides of this inequality with brute-force, and get following condition:

$$\begin{aligned} &k(k+1)C_1C_2 + k(k+1)C_1x^2 - (k+1)C_1^2C_2 - (k+1)C_1^2x^2 \\ &- kC_1^3 - 2kC_1^2x - kC_1x^2 + C_1^4 + 2C_1^3x + C_1^2x^2 \\ &> k(k+1)C_1C_2 + k(k+1)C_2x - kC_1^2C_2 - 2kC_1C_2x \\ &- kC_2x^2 - (k+1)C_1^3 + C_1^4 + C_1^3x - (k+1)C_1^2x + C_1^3x + C_1^2x^2 \end{aligned} \quad (94)$$

which is equivalent to:

$$(k^2C_1 - (k+1)C_1^2 + kC_2)x^2 - ((k-1)C_1^2 + 2kC_1C_2 + k(k+1)C_2)x + C_1^3 - C_1^2C_2 > 0 \quad (95)$$

A.6 Proof of Lemma 1

Proof. First, we will continue to apply the idea of expansion in the proof of variance part of Theorem 1. However, the proof in the Theorem 1 can't apply directly because the order of $\mathbb{E}[(z_i - c)(z_k - c)z_j z_l]$ increases from $\Theta(1/n)$ to $\Theta(1)$, when $w \neq c$. These two cases are:

1. Only $j = l$ holds, with i, j , and k being distinct.
2. i, j, k, l are all distinct.

For the first case, we resort to the third part of Assumption 1:

$$\sum_{i,j,k} B_{ij} B_{kj} = \sum_j (\sum_i B_{ij})^2 = O(n) \quad (96)$$

For the second case, we will prove that the two coefficients of term $(\sum_{ij} B_{ij})^2$ in the expression of $\text{Var}((\mathbf{z} - w\mathbf{1})^T B\mathbf{z})$ can cancel out. Namely, we will prove:

$$\mathbb{E}[(z_i - w)(z_k - w)z_j z_l] - (\mathbb{E}[(\mathbf{z} - w\mathbf{1})^T B\mathbf{z}] / \text{trace}(\mathbf{1}\mathbf{1}^T B))^2 = O(\frac{1}{n}) \quad (97)$$

for the case i, j, k, l are not equal to each other.

Notice that, for $s = 1, 2, 3$, we have:

$$\frac{d-s}{n-s} = c + O(\frac{1}{n}) \quad (98)$$

On one hand,

$$\begin{aligned} \mathbb{E}[(z_i - w)(z_k - w)z_j z_l] &= \mathbb{E}[(z_i - w)(z_k - w) \mid z_j = z_l = 1] \left(c^2 + O(\frac{1}{n}) \right) \\ &= (c - w)^2 c^2 + O(\frac{1}{n}) \end{aligned} \quad (99)$$

On the other hand,

$$\begin{aligned} \frac{\mathbb{E}[(\mathbf{z} - w\mathbf{1})^T B\mathbf{z}]}{\text{trace}(\mathbf{1}\mathbf{1}^T B)} &= \frac{\text{trace}(\mathbb{E}[\mathbf{z}(\mathbf{z} - w\mathbf{1})^T] B)}{\text{trace}(\mathbf{1}\mathbf{1}^T B)} \\ &= \frac{\text{trace}((\mathbb{E}[\mathbf{z}\mathbf{z}^T] - cw\mathbf{1}\mathbf{1}^T)B)}{\text{trace}(\mathbf{1}\mathbf{1}^T B)} \\ &= c(c - w) + O(\frac{1}{n}) \end{aligned} \quad (100)$$

In the last equation, we again utilize $B_{ii} = 0$ for all unit $i \in [n]$. Combine two equations above, we successfully control the order of coefficient of term $(\sum_{ij} B_{ij})^2$, in the expression of concerned variance $\text{Var}((\mathbf{z} - w\mathbf{1})^T B\mathbf{z})$.

For other three cases of $\mathbb{E}[(z_i - c)(z_k - c)z_j z_l]$, the proof of Theorem 1 can be utilized directly here, because $\mathbb{E}[(z_i - c)(z_k - c)z_j z_l] = \Theta(1)$ there, and the order of this term can't exceed constant no matter what value w takes. Therefore, we finish the proof.

A.7 Proof of Theorem 4

Proof. The result with independent T experiments is a direct extension of Lemma 1. In fact, with Lemma 1, we can conclude that

$$\text{Var} \left(\sum_{t=1}^T \left(\mathbf{z}_t - \frac{\sum_{k=1}^T c_k}{T} \mathbf{1} \right)^T B\mathbf{z}_t \right) = \sum_{t=1}^T \text{Var} \left(\left(\mathbf{z}_t - \frac{\sum_{k=1}^T c_k}{T} \mathbf{1} \right)^T B\mathbf{z}_t \right) = O(\frac{1}{n}) \quad (101)$$

On the other hand, the order of variance introduced by ϵ is always $\Theta(1/n)$, and the concerned variance is the sum of these non-negative variance terms. Therefore, we can conclude that

$$\text{Var}(\hat{\tau})/\beta_2^2 = \Theta\left(\frac{1}{n}\right) \quad (102)$$

A.8 Proof of Theorem 5

Proof. Based on the Lemma 1, the remaining work is bounding the sum of covariance terms. We have:

$$\begin{aligned} \text{Var}\left(\sum_{t=1}^T (\mathbf{z}_t - \frac{\sum_{k=1}^T c_k}{T} \mathbf{1})^T B \mathbf{z}_t\right) &= \sum_{t=1}^T \text{Var}\left((\mathbf{z}_t - \frac{\sum_{k=1}^T c_k}{T} \mathbf{1})^T B \mathbf{z}_t\right) \\ &\quad + 2 \sum_{t_1 < t_2} \text{Cov}[(\mathbf{z}_{t_1} - \frac{\sum_{k=1}^T c_k}{T} \mathbf{1})^T B \mathbf{z}_{t_1}, (\mathbf{z}_{t_2} - \frac{\sum_{k=1}^T c_k}{T} \mathbf{1})^T B \mathbf{z}_{t_2}] \end{aligned} \quad (103)$$

For simplicity, we use \mathbf{u}, \mathbf{v} to denote $\mathbf{z}_{t_1}, \mathbf{z}_{t_2}$, respectively, and use $w = \sum_{t=1}^T c_t/T$. We continue to expand the covariance term, and get:

$$\sum_{i,j,k,l} B_{ij} B_{kl} (\mathbb{E}[(u_i - w) u_j (v_k - w) v_l] - \mathbb{E}[(u_i - w) u_j] \mathbb{E}[(v_k - w) v_l]) \quad (104)$$

Correspondingly, we need to discuss the order of the this term in five cases, as well as that in the Appendix A.1. Similarly, for the first four cases (except for the case where i, j, k, l are not equal to each other), we allow for:

$$\mathbb{E}[(u_i - w) u_j (v_k - w) v_l] - \mathbb{E}[(u_i - w) u_j] \mathbb{E}[(v_k - w) v_l] = \Theta(1) \quad (105)$$

Therefore, we only need to prove:

$$\mathbb{E}[(u_i - w) u_j (v_k - w) v_l] - \mathbb{E}[(u_i - w) u_j] \mathbb{E}[(v_k - w) v_l] = O\left(\frac{1}{n}\right) \quad (106)$$

when i, j, k, l are not equal to each other.

Since \mathbf{u} is the treatment vector that is assigned before \mathbf{v} , we should first condition on u_i, u_j .

$$\begin{aligned} \mathbb{E}[(u_i - w) u_j (v_k - w) v_l] &= \left(c_{t_1}^2 + O\left(\frac{1}{n}\right)\right) (1-w) \mathbb{E}[(v_k - w) v_l \mid u_i = u_j = 1] \\ &\quad - \left(c_{t_1}(1 - c_{t_1}) + O\left(\frac{1}{n}\right)\right) w \mathbb{E}[(v_k - w) v_l \mid u_j = 1] \\ &= (1-w) c_{t_1}^2 (c_{t_2} - w) c_{t_2} - w c_{t_1} (1 - c_{t_1}) (c_{t_2} - w) c_{t_2} + O\left(\frac{1}{n}\right) \\ &= (c_{t_1} - w) c_{t_1} (c_{t_2} - w) c_{t_2} + O\left(\frac{1}{n}\right) \end{aligned} \quad (107)$$

On the other hand, it is easy to check that

$$\mathbb{E}[(u_i - w)u_j] \mathbb{E}[(v_k - w)v_l] = (c_{t_1} - w)c_{t_1}(c_{t_2} - w)c_{t_2} + O\left(\frac{1}{n}\right) \quad (108)$$

Thus, we finish the proof.

Remark. In fact, the covariance term in other four cases are likely of constant order. For example, we check the case where only $j = l$ holds:

$$\begin{aligned} \mathbb{E}[(u_i - w)u_j(v_k - w)v_l] &= \mathbb{E}[(u_i - w)u_j(v_k - w)v_j] \\ &= c_{t_1} \mathbb{E}[(u_i - w)(v_k - w)v_j \mid u_j = 1] \\ &= c_{t_1} \left(c_{t_1} - w + O\left(\frac{1}{n}\right) \right) \left(c_{t_2} - w + O\left(\frac{1}{n}\right) \right) \\ &= c_{t_1}(c_{t_1} - w)(c_{t_2} - w) + O\left(\frac{1}{n}\right) \end{aligned} \quad (109)$$

Therefore, in this case, the value of covariance term

$$\begin{aligned} &\mathbb{E}[(u_i - w)u_j(v_k - w)v_l] - \mathbb{E}[(u_i - w)u_j] \mathbb{E}[(v_k - w)v_l] \\ &= c_{t_1}(c_{t_1} - w)(c_{t_2} - w) - c_{t_1}c_{t_2}(c_{t_1} - w)(c_{t_2} - w) + O\left(\frac{1}{n}\right) \\ &= \Theta(1) \end{aligned} \quad (110)$$

if $c_{t_1} > 0$ and $c_{t_2} < 1$. Therefore, the third part of Assumption 1 is still necessary here.

B Simulation Details

B.1 Parameters

The used architecture of GNN is composed of three layers of ChebConv, with input dimension, output dimension, and filter size $(2, 16, 2), (16, 16, 1), (16, 1, 1)$, respectively.

We comment that such a size of parameters is enough to guarantee that the training loss decreases to the level lower than 0.2, in most cases. Moreover, if we continue to increase the size of parameters, e.g. increase the size of filters, the performance of GNN trained on single experimental data with treatment proportion $c = 0.5$ would become worse, which indicates that the volume of one graph can not support better performance. Through back-and-forth adjustment, we finally determine this set of parameters of network architecture.

Specifically, we only select the treatment of unit z_i and its degree \deg_i as initial feature for each unit i .

Moreover, we implement Monte Carlo simulations with 1,000 continuous random seeds, which control the treatment allocation. We fix another random seed that controls the initialization of the graph neural network, among all cases examined in our paper. If such a random seed also changes in a Monte

Carlo simulation, empirically, there would be about ten percent of instances where the model falls into a local minimum in the very early stage.

Other miscellaneous parameters are presented as below:

1. Resolution of clustering: 10
2. Number of clusters: 192
3. Activation function: ReLU
4. Number of training epochs: 400
5. Optimizer: Adam with learning rate 0.004 and momentum coefficient (betas) 0.9,0.999.

B.2 Performance of Linear Regression Estimator

In this section, we supplement the statistical performance of linear regression estimator, as shown in Figure 1 and 5 before. Similar to the setting of the main paper, we fix the randomization scheme as complete randomization with staggered rollout. We consider treatment proportions $(c_1, c_2, \dots, c_5) = (2\%, 5\%, 10\%, 25\%, 50\%)$ in the ramp-up process and consider the training data composed by $t = 1, 2, 3, 4, 5$ steps, corresponding to the treatment proportions (c_{6-t}, \dots, c_5) . The detailed result is presented in Table 19.

Table 19: The performance of linear regression estimator

level metric rounds	Unit			Cluster		
	Bias	Std	MSE	Bias	Std	MSE
	$t = 1$	$t = 2$	$t = 3$	$t = 4$	$t = 5$	
	-1.000	0.004	1.000	-0.595	0.010	0.354
	-0.933	0.003	0.871	-0.554	0.019	0.307
	-0.866	0.003	0.750	-0.518	0.027	0.269
	-0.824	0.003	0.680	-0.493	0.028	0.244
	-0.792	0.003	0.628	-0.471	0.031	0.223

We observe that the bias reductions introduced by merging compared to the case of $t = 1$ verify

B.3 Performance of Lagrangian Interpolation Estimator

We then discuss the performance Lagrangian interpolation estimator proposed in [20]. As a system-level estimator that is agnostic to the microstructure of the graph, it only approximates the one-dimensional function $\bar{Y}(p)$, namely, the mean outcome function w.r.t. the treatment proportion p , with unit-level independent Bernoulli randomization.

In fact, such a Lagrangian interpolation estimator specifies the polynomial basis that incorporates the following interference term:

$$\sum_{\ell=1}^{\beta} w_{\ell} \left(\frac{\sum_{j \in \mathcal{N}_i} \tilde{c}_{ij} z_j}{\sum_{j \in \mathcal{N}_i} \tilde{c}_{ij}} \right)^{\ell} \quad (111)$$

where \tilde{c}_{ij} is the coefficient that characterizes the influence from unit j to unit i , and w_{ℓ} is the intensity of interaction of ℓ -th order.

In most of the potential outcome models discussed in related works, the value of true GATE is actually not concerned with the topology of the graph. Therefore, extrapolating the mean outcome at $p = 1$ is feasible in these cases. We comment that an important reason for this phenomenon is the scarcity of unit-specific covariates, such as demographics as nodal features, and interaction terms composed of covariate and treatment.

The basic linear potential outcome model and linear potential outcome model with a quadratic interference term discussed in our simulation study belong to this category. As a comparison, the idea of the neural network is constructing an adaptive basis for function approximation. Namely, our methodology can easily incorporate the nodal covariate and complex interaction model in reality, as validated by the successful application of GNN in practice.

We further remark that flexibly learning the microstructure model becomes feasible because we leverage the information of all nodes. Otherwise, scarcity of data generally limits the application of neural networks.

In the following, we provide some examples. The main message is that both the **exact** knowledge on order of interaction, i.e. β , and the **realizability** through polynomial basis, is important for achieving good performance through this estimator, though both of these two conditions are vulnerable in practice. We continue to use the notations in the main paper.

We first examine the case of the classic linear potential outcome model that is formulated in section 5.2. We have $\beta = 1$ in this case. First, we consider $c_1 = 0, c_2 = 50\%$, the performance triplet (Bias, Std, MSE) is $(0.003, 0.018, 0.000)$, which indicates a great performance. However, when we increase the number of steps, i.e. $c_1 = 0, c_2 = 25\%, c_3 = 50\%$, the performance triplet changes to $(-0.012, 0.079, 0.006)$. Moreover, when we continue to increase the number of steps i.e. $c_1 = 0, c_2 = 10\%, c_3 = 25\%, c_4 = 50\%$, the performance triplet changes to $(0.092, 0.547, 0.308)$, which is much worse than expected.

Next, we examine the scenario of quadratic interference, as formulated in section 5.4. We repeat the three cases above and get corresponding performance triplets: $(-0.451, 0.018, 0.204)$, $(-0.010, 0.069, 0.005)$, and $(0.075, 0.390, 0.158)$. In this scenario, we have $\beta = 2$. Through the two examples above, we can find that the good performance of this estimator heavily relies on the **exact** knowledge on such β .

We then examine the scenario of square root interference, which is beyond the space spanned by a polynomial basis. Similarly, we repeat the three cases above and get corresponding performance triplets: $(0.385, 0.016, 0.148)$, $(-0.654, 0.075, 0.434)$, and $(3.323, 0.631, 11.443)$. We observe that the performance becomes always bad and extremely unstable, which can even worsen with the increase of times of experiments.